

# **Diatom inferred aquatic impacts of the mid-Holocene eruption of Mount Mazama, Oregon**

Joanne Egan<sup>1</sup>, Timothy E.H. Allott<sup>2</sup>, Jeffrey J. Blackford<sup>3</sup>

<sup>1</sup> Department of Geography, Edge Hill University, St Helens Road, Ormskirk, Lancashire, L39 4QP.

Corresponding author email: [eganj@edgehill.ac.uk](mailto:eganj@edgehill.ac.uk), telephone: 01695 584462

<sup>2</sup> Department of Geography, School of Environment, Education and Development, University of Manchester, Oxford Road, Manchester, M13 9PL, UK.

<sup>3</sup> Department of Geography, Environment and Earth Sciences, University of Hull, Cottingham Road, Hull, HU6 7RX, UK

## **ABSTRACT**

High-resolution diatom stratigraphies from mid-Holocene sediments taken from fringe and central locations in Moss Lake, a small lake in the foothills of the Cascade Range, Washington, have been analysed to investigate the impacts (and duration) of tephra deposition on the aquatic ecosystem. Up to 50 mm of tephra was deposited from the climactic eruption of Mount Mazama 7958-7795 cal yr BP, with coincident changes in the aquatic ecosystem. The diatom response from both cores indicates a change in habitat type following blanket tephra deposition, with a decline in tychoplanktonic *Fragilaria brevistriata* and *Staurosira venter* and epiphytic diatom taxa indicating a reduction in aquatic macrophyte abundance. Additionally, the central core shows an increase in tychoplanktonic *Aulacoseira* taxa, interpreted as a response to increased silica availability following tephra deposition. However, partial redundancy analysis provides only limited evidence of direct effects from

the tephra deposition, and only from the central core, but significant effects from underlying environmental changes associated with climatic and lake development processes. The analyses highlight the importance of duplicate analyses (fringe and central cores) and vigorous statistical analyses for the robust evaluation of aquatic ecosystem change.

Keywords: Tephra impact, Diatoms, Mazama, Redundancy analysis, Holocene, Volcano

## INTRODUCTION

Volcanic eruptions may have major impacts on ecosystems, and although the proximal impacts are generally well understood, the distal impacts of distal tephra deposition are not well defined (see Payne and Egan, 2017 for a review). The ‘fine’ to ‘very fine’ (between <30 and 100  $\mu\text{m}$ ) class size of ash is of particular importance in this context as they have the longest atmospheric residence times, travel the furthest distance and carry the most toxic volatiles (Payne and Blackford, 2008), which makes them particularly hazardous to the environment (Rose and Durant, 2009). The impact of volcanic eruptions on climate and ecosystems can be detrimental. This can be through direct climatic perturbations (Mass and Portman, 1989; McCormick *et al.*, 1995; Zielinski, 2000; Stoffel *et al.*, 2015), though such effects usually last only 1-3 years (McCormick *et al.*, 1995; Zdanowicz *et al.*, 1999). It is the effects of tephra deposition on different receiving environments that may have longer-term, decadal to centennial (Barker *et al.*, 2000; Telford *et al.*, 2004; Blackford *et al.*, 2014; Egan *et al.*, 2016) and even millennial (Bradbury *et al.*, 2004) effects and are more ambiguous in nature. Focussing on the aquatic effects of tephra deposition, this paper aims to enhance our understanding of tephra impacts.

Egan *et al.*, (2016) conducted a study on the terrestrial impacts of the tephra deposited by the Plinian eruption of Mount Mazama, Cascade Range, 7682-7584 cal yr BP (95.4% probability range) (Egan *et al.*, 2015). Mount Mazama ejected nearly 50 km<sup>3</sup> of rhyodacitic magma into the atmosphere (ten times as much as the 1980 eruption of Mount St Helens), and deposited ash over an area of approximately 1.7x10<sup>6</sup> km<sup>2</sup> (Zdanowicz *et al.*, 1999) in a predominantly north-easterly direction (Figure 1). Egan *et al.*, (2016) reported a significant local impact on the terrestrial environment surrounding Moss Lake, Washington, with decreases in the open habitat vegetation. Building on the potential impacts from the Mazama tephra deposit here, we are now primarily interested in the nature and duration of the aquatic impacts, which Egan *et al.*, (2016) did not address. Egan *et al.*, (2016) highlighted the importance of multiple cores as their analyses revealed a local terrestrial impact but no regional impact. Here we assess both shallow and deep cores from Moss Lake through the use of high resolution diatom analyses to determine the physiochemical effects of tephra deposition on the aquatic environment.

Tephra can impact aquatic systems physically, biologically and chemically. The direct input of tephra may instantly kill aquatic life as tephra may get stuck in fish gills and can be toxic to aquatic organisms (Ayris and Delmelle, 2012; Lallement *et al.*, 2016). Physically tephra can make the water more turbid (Lallement *et al.*, 2016), reduce light infiltration (Abella, 1988), alter drainage patterns and water flow (Lallement *et al.*, 2016) and alter habitat availability with the death of aquatic plants reducing epiphytic species and newly deposited tephra allowing epipelagic algae to colonise (Telford *et al.*, 2004). Such physical changes can have implications for the biology as fish and algae can be displaced as their habitat is destroyed, and the changes in light penetration can reduce photosynthetic activity thus altering oxygen levels in the water. Chemically the aquatic system can be changed by increased concentrations of heavy metals (Power *et al.*, 2011) or by decreasing the pH

73 through the influx of associated sulphuric acid (Birks and Lotter, 1994). Silica is also added  
74 to the aquatic system. Whilst this is an instant input, Telford *et al.*, (2004) state that it  
75 dissolves slowly, and even when the tephra is deposited onto the lake bed, the silica will still  
76 be released, which provides a steady influx of silica to the aquatic system. Some diatom  
77 species are likely to be competitively advantaged and response positively to the increased  
78 silica input (Telford *et al.*, 2004). An additional effect of tephra deposition in lakes is that a  
79 thick tephra layer creates an impermeable barrier over the lake's sediment, preventing the  
80 regeneration of nutrients such as phosphorus (Barker *et al.*, 2000, 2003). Tephra presents a  
81 physical barrier to the transport of phosphorus into the water column by preventing re-  
82 suspension of the sediment by bioturbation and wave action, as well as a barrier to  
83 phosphorus diffusion depending on its thickness. Any changes in the chemical status of the  
84 lake would impact on the biological and thus physical characteristics of the aquatic system, as  
85 these three components are interconnected.

86 A recent study has assessed the aquatic impacts of tephra fallout from the rift zone eruption  
87 of the Puyehue Cordon-Caulle volcanic complex, Patagonia in 2011, and reported habitat  
88 loss, changes in morphology of the main channels, increases of turbidity and a sharp decline  
89 in salmonid fish densities (Lallement *et al.*, 2016). These impacts persisted for 30 months  
90 after the initial eruption, with some evidence that recovery is underway but uncertainties exist  
91 as to whether the channels and their fish assemblages will ever return to the pre-impact  
92 conditions. Continuous monitoring in active volcanic terrains like this example is rare and  
93 few have the decadal durations required to record longer-term trends, thus much less is  
94 known about the long-term impacts on aquatic ecosystems.

95 Palaeoenvironmental records have been used in several studies to successfully infer long-  
96 term impacts of volcanic eruptions and subsequent recovery. Diatoms are frequently used as a

proxy for tephra impacts in lakes as these algae are affected first due to their high sensitivity and rapid responses, and their preservation means that longer term impacts can be assessed (Abella, 1988; Birks and Lotter, 1994; Barker *et al.*, 2000; Colman *et al.*, 2004; Telford *et al.*, 2004). They are particularly useful for determining chemical and physical changes in the aquatic system.

Six studies have assessed the aquatic impacts of tephra deposition from Mount Mazama (Blinman *et al.*, 1979; Abella, 1988; Hickman and Reasoner, 1994; Bradbury *et al.*, 2004; Stone, 2005). The studies reported varying impacts including: a decrease of pH (Bradbury *et al.*, 2004), increase of salinity (Heinrichs *et al.*, 1999; Bradbury *et al.*, 2004), a change in the Si:P ratio (Abella, 1988; Hickman and Reasoner, 1994) and changes in water chemistry that lasted nearly a millennium (Stone, 2005). Most of these lake systems are large in size and highly productive (Abella, 1988; Bradbury *et al.*, 2004; Stone, 2005), and therefore not typical or representative of the majority of lakes in the Cascade region which are smaller and nutrient poor (Hickman and Reasoner, 1994; Heinrichs *et al.*, 1999). Evaluations are therefore needed from such systems, which may be more sensitive to disturbance. This study provides an assessment of the distal impacts of tephra deposition on the aquatic ecosystem of a small, oligotrophic lake system within the foothills of the Cascades.

## STUDY AREA

The Mazama tephra is of great stratigraphic importance as the climactic eruption of Mount Mazama was a high magnitude event producing the most significant tephra fall of the Holocene in North America and it has been identified at Moss Lake. Moss Lake (47°41.60N, 121°50.81W – Datum used: WGS 84) is 500 km north of Crater Lake (the site of the Mount

Mazama eruptions) allowing distal impacts to be assessed. Moss Lake is located in a mixed conifer forest within the Tolt River basin in King County in the Cascade foothills at an elevation of 158 m (Figure 1). The lake has a diameter of approximately 200 m with a maximum depth of 4.5 m. Moss Lake resides in a shallow basin within a broad fluted basal till plain that was deposited during the Vashon Stade (~18,000-16,500 cal yr BP at the site; Porter and Swanson, 1998). This till sheet overlies glaciomarine drift and outwash deposits (Dragovich *et al.*, 2002).

During the time of the deposition event Moss Lake included an extensive shallow water system, and today the lake is surrounded by a reed swamp (see Figure 1, inset in top left) underlain by lake sediments. This lake setting is ideal for the study with stratigraphies from both a core from the fringing reed swamp, representative of the Holocene shallow water system and potentially dominated by benthic taxa, as well as a deep water core from the centre of the lake, potentially with higher representation of planktonic and tychoplanktonic taxa. Moss Lake is a freshwater, oligotrophic system with a weakly acidic-neutral pH of 6 and low conductivity of 14-22  $\mu\text{S cm}^{-1}$ . Water chemistry analyses indicate the lake has a low concentration of calcium suggesting that it has a low buffering capacity and may be sensitive to acid deposition from volcanic events (for present day water chemistry see Supplementary Table 1). This study will add further detail to current knowledge regarding impacts of tephra deposition, and being in such close proximity to other major volcanoes such as Glacier Peak, Mount St Helens and Mount Rainier it is essential that as much research is done in this area as possible.

## MATERIALS AND METHODS

## Core collection

To elucidate true volcanic impacts cores were taken from the lake fringe (MLF) and a central part of the lake (MLC) representative of a shallow water and deep water lake system. MLC was collected from the deepest point of Moss lake, determined with an echo sounder, using a modified Livingstone corer. A second core was extracted from the fringe (MLF) using a Russian corer. The cores were placed in guttering, wrapped in cling film and stored in the cold room (dark, 2-4°C) at The University of Manchester. As the focus of this paper is the impact of tephra deposition, analyses concentrate on sediments above and below the Mazama tephra deposit, not the whole Holocene record.

## Stratigraphic analyses and radiocarbon dating

Data reported here for the stratigraphy and chronology are taken from Egan *et al.*, (2016) where further details of the methods can be found. To summarise, we measured the organic matter content, carbonates, particle size and magnetic susceptibility. For the analyses here, we report the data from the samples taken every 5 mm above, below, and through the tephra layer (magnetic susceptibility was measured every 10 mm). Particle size analysis was carried out in order to assist with the determination of the tephra layer boundary in MLF, as it was not distinct. Samples were taken every 10 mm (every 5 mm through the tephra layer).

The Mazama tephra layer has previously been geochemically identified on the JEOL-JXA8600 electron microprobe at the Research Laboratory for Archaeology and the History of Art, University of Oxford (Egan *et al.*, 2016).

AMS radiocarbon dates were obtained for both cores as discussed in the previous work in Egan *et al.*, (2016). Radiocarbon dating was carried out on bulk sediments as there were no identifiable macrofossils or macrocharcoal fragments. The low sedimentary carbonate content indicates that hard water reservoir effects are unlikely. Originally, eight radiocarbon dates were obtained for MLC (Egan *et al.*, 2016), here we present four of those ages that focus directly on the Mount Mazama deposit. Radiocarbon dates were calibrated to calendar years (cal yr BP) using OxCal v.4.2.4 (Bronk Ramsey, 2014), and the IntCal13 calibration curve (Reimer *et al.*, 2013). A full chronology was determined with an age-depth model. We used a *P\_sequence* deposition model in OxCal v.4.2.4. To account for the 40 mm thick tephra layer, representing instantaneous deposition an “event free depth scale” was included (Staff *et al.*, 2011). Three radiocarbon ages are reported for MLF, however an age reversal was present so an accurate chronology could not be determined.

181

## 182 **Diatom analysis**

183

High resolution samples (1 mm contiguous samples for MLF and 5 mm contiguous samples for MLC) were taken before and after the tephra layers. The age-depth model for MLC suggests these samples represent approximately 10-20 years. The high resolution sampling was done by slicing the sediment with a scalpel and avoiding areas of tephra penetration outside of the primary tephra layer. Diatom preparation followed the standard procedure by Battarbee (1986), and followed Renberg's (1990) recommendation of bulk preparation using a water-bath. Approximately 0.03 g of dry sediment was digested in 5 ml of 30% hydrogen



peroxide, 1-2 drops of hydrochloric acid were added to eliminate any remaining hydrogen peroxide and carbonates. Samples were washed several times and weak ammonia was added on the final wash to keep clays in suspension and to prevent diatom clumping. Microspheres were added to determine diatom concentration (Battarbee and Kneen, 1982). The concentration of microspheres added was 2 ml of  $5.01 \times 10^6$  per 0.01 g dry weight of sediment. Samples were mounted on the microscope slide using Naphrax<sup>®</sup> and were identified and counted at 1000x magnification. Identification was through the website “Diatoms of the United States” (Spaulding, 2014) and identification keys (Krammer and Lange-Bertalot, 1991, 1999a, 1999b). At least 300 diatom frustules were counted.

Diatom diagrams presented here show the percentages of total frustules. The summary diagram is based on habitat preference determined primarily from “Diatoms of the United States” (Spaulding, 2014) and Kelly *et al.*, (2005). Diatom zonation was used not only to assist with qualitative analyses, but also as a quantitative tool, as the zones determined represent significant changes in the assemblage. To determine statistically significant changes optimal splitting by information content was used (Bennett, 1996), and the number of significant zones was determined through the use of the Broken-Stick model (Bennett, 1996). Diatom diagrams and the zonation were created using Psimpoll v.4.27 (Bennett, 2007).

#### **Ordination and associated significance tests**

Ordination was used to test for significant changes in the diatom record following the deposition of tephra, evaluating the significance of the impact of each tephra relative to and independently from additional environmental variables chosen to account for underlying

environmental trends. Detrended Correspondence Analysis (DCA) (Hill and Gauch, 1980) was used initially to estimate the length of the gradients in the biostratigraphical data sets (in standard deviation units). The diatom assemblages have short gradients ( $<1.7$  SD), and consequently linear ordination methods were employed (Leps and Šmilauer, 2014). Principal Component Analysis (PCA) (Orloci, 1966) was then used to describe the relationships between different diatom species and samples.

Partial Redundancy Analysis (RDA) (ter Braak and Prentice, 1988; Rao, 1964), a constrained form of PCA, was used to determine how much of the variation is explained by the environmental variables and their significance. Log transformation and double centring of the samples and environmental variables were used to allow for the closed compositional disposition of the data. In order to test the significance of each environmental variable independent from the other two co-variables, timeseries restricted Monte Carlo permutation tests used for stratigraphically ordered data (ter Braak and Šmilauer, 2012) were completed with 999 permutations. The significance test compares eigenvalues for the first RDA axes of the diatom assemblages. The statistical program used was Canoco v5 (ter Braak and Šmilauer, 2012).

The influence of three independent environmental variables (tephra, LOI and core depth) on the diatom data was evaluated using direct ordination (partial RDA). Observed changes in the diatom assemblages around the time of volcanic events may have been a response to tephra deposition. This effect is modelled as an exponential decay function through time (Lotter and Birks, 1993; Birks and Lotter, 1994; Barker *et al.*, 2000; Lotter and Anderson, 2012; Blackford *et al.*, 2014). Prior to deposition of tephra the tephra explanatory variable was given a value of 0. At the time of tephra deposition, the value for ash was given an arbitrary value of 100, and after deposition the value of ash decreased exponentially  $x^{-\alpha t}$ , where  $\alpha$  is the decay coefficient and  $t$  is sample time ( $f$ = depth) since tephra deposition. Three models

(different decay coefficients) were used for the diatom assemblage from MLC to reflect different potential recovery times. Model 1 had a decay coefficient of 0.8 to reflect the longest recovery time of approximately 500 years, with most recovery having happened within approximately 200-250 years, model 2 had a decay coefficient of 0.5 to reflect medium duration or recovery of approximately 200 years, with most recovery having happened within approximately 100 years, and model 3 had a decay coefficient of 0.1 to reflect the shortest recovery time of approximately 80 years, with most recovery having happened within approximately 20 years. An ongoing study in an alpine lake in Washington has found strong evidence that tephra from Mount Mazama exerted significant influence on sedimentation dynamics for up to 500 years post deposition (Wershow, pers. comm.), thus the timeframes suggested by the models is realistic. For MLC all models were used as there was variation within the results. However, for MLF there was little difference in the results, so the decay coefficient used for this assemblage was 0.5, model 2. LOI was the second environmental variable representing the inflow of exogenic mineral materials, which would be associated with low organic matter content, and local environmental change. LOI was corrected for tephra by interpolating values for the samples containing tephra, so there was no influence of the tephra itself on this variable. The third variable was depth, as a surrogate for age to represent directional change during the period of tephra deposition associated with climate change or successional processes.

## **RESULTS**

### **Stratigraphy**

A wider stratigraphy for MLC is reported in Egan *et al.*, (2016), Figure 2 displays the stratigraphy of MLC around the time of Mazama tephra deposition (MLC-T324), the focus here. Figure 2 shows a shift from silty gyttja in sediment unit MLCs-1 to organic peaty silt in MLCs-2. LOI decreases and drops to 5% upon the deposition of the Mazama tephra. Organic matter content increases steadily after this in MLCs-2. Magnetic susceptibility increases upon tephra deposition from  $0.2 \times 10^{-7}$  SI to  $59 \times 10^{-7}$  SI. Carbonate content values are consistently below 0.01%. Figure 3 illustrates the MLF stratigraphy (again, a wider stratigraphy is presented in Egan *et al.*, (2016)). Particle size analysis was used to determine the boundary of tephra deposition and shows a peak in coarse and fine sand between 158-153 cm, indicative of the tephra boundary. At the base of sediment unit MLFs-1 organic sandy silts dominate with low LOI (~25%) and magnetic susceptibility values of  $3.5 \times 10^{-6}$  SI. Within the Mazama tephra deposit (MLF-T158) LOI further decreases to ~17% and magnetic susceptibility peaks to  $94 \times 10^{-6}$  SI. In MLFs-2 silty peats develop with an increasing LOI from ~20% to ~80% and generally low magnetic susceptibility of  $1-7 \times 10^{-6}$  SI. A silt unit is present from 146-132 cm. There is a brief increase of magnetic susceptibility (to  $45 \times 10^{-6}$  SI) and particle size at around 120 cm where there is a coarse sand deposit. Carbonate content values are consistently below 0.03%.

## **Radiocarbon**

The MLC sediment record extends back to the late Pleistocene, 16,294-12,789 cal yr BP, reported previously in Egan *et al.*, (2016) and is well constrained. However, the focus here is on the aquatic impact of the Mazama tephra deposit. Thus the record presented here spans the time period ~8400 cal yr BP to ~7100 cal yr BP (Table 1, Figure 4). The three radiocarbon

dates for MLF demonstrated an age reversal in the top two samples and was confirmed by re-analysis of the samples (Supplementary Table 3). The dates therefore cannot be used in the analyses, but are provided to demonstrate that MLF-T158 is within the right time period as the sediments below the tephra have a calibrated age range of 7958-7795 cal yr BP (95.4% probability range). Therefore, further up the core within the tephra layer the age is likely to be younger and within the previously published age range of 7682-7584 cal yr BP (95.4% probability range) (Egan *et al.*, 2015).

## Diatoms

MLC has high proportions of planktonic *Discostella pseudostelligera* (up to 60%) and low proportions of epipelagic (~10%) and epiphytic (<5%) taxa. *Discostella pseudostelligera* is dominant throughout the assemblage. Figure 5 displays the diatom assemblage for MLC and Table 2 summarises the main changes in the diatom assemblage around the time of Mazama tephra deposition. Three zones have been identified. The first zone (C1) includes the pre-tephra assemblage and the tephra deposit itself. The transition into the second zone (C2) starts above the tephra deposit at 320.8 cm, the third zone (C3) starts at 313.7 cm. The zonation suggests tephra deposition from Mount Mazama caused marked change in the aquatic environment with clear differences in the assemblages before and after tephra deposition. In zone C1 *Discostella pseudostelligera* increasingly dominates from 40% to 60%, and tychoplanktonic species *Fragilaria brevistriata* and *Staurosira venter* decrease from 15% to <5% and 25% to <5% respectively. When tephra is deposited *Aulacoseira* taxa increase by a small percentage (<5%) and *Fragilaria brevistriata* and *Staurosira venter* decrease further to <5%. In zone C2 *Discostella pseudostelligera* still dominates but

decreases from 60% to 40%, whilst tychoplanktonic taxa increase overall from 30% to 45%. Zone C3 consists of a higher abundance of *Discostella pseudostelligera* (up to 70%), *Aulacoseira* taxa (>20%), *Fragilaria brevistriata* (up to 20%) and *Staurosira venter* (up to 20%) than in zone C2.

MLF (Figure 6, Table 2) has a very different assemblage to MLC, in particular lower proportions of planktonic *Discostella pseudostelligera* (<5%) and higher proportions of epipellic (up to 50%) and epiphytic (up to 50%) taxa. The assemblage is dominated by epiphytic taxa throughout most of the profile, specifically *Eunotia soleirolii*, *Encyonema mesianum* and *Gomphonema gracile*. Tychoplanktonic taxa, specifically *Aulacoseira lirata*, have a high abundance (up to 55%) before the tephra deposition event, and epipellic taxa are high in abundance (up to 50%) after the tephra event, notably *Brachysira brebissonii* increasing from <5% to 20%. Two zones have been identified, and the split is during the time of Mazama tephra deposition, suggesting there was a marked assemblage change. Before tephra deposition in zone F1 epiphytic taxa dominate (up to 40%), in particular *Gomphonema gracile* and *Eunotia soleirolii* along with tychoplanktonic *Aulacoseira lirata*, *Aulacoseira alpigena*, *Fragilaria brevistriata* and *Staurosira venter*. Epipellic taxa increase after tephra deposition from 20% to 50%. In zone F2 epipellic species, especially *Brachysira brebissonii* dominate. Tychoplanktonic and epiphytic taxa are in lower abundance than in zone F1 decreasing from up to 50% to 10% and 50% to 40% respectively.

## Ordination and significance tests (PCA and partial RDA)

### Principal Components Analysis

The gradients in both data sets for MLF and MLC had lengths of 1.1 and 0.7 SD units respectively. These short gradient lengths show that there was restricted turn-over in the diatom data as a standard deviation unit length of 4 would be indicative of complete species turn-over (Lepš and Smilauer, 2014).

Moss Lake Central (MLC) has two important PCA gradients (Figure 5); PCA axis 1 accounts for 26% of the variance and PCA axis 2 explains a further 21% of the variance. PCA axis 1 is associated with short term variations in tychoplanktonic taxa (Figure 5) with a shift from positive to negative sample scores in zone C1, until Mazama tephra deposition in zone C2 where sample scores increase and become positive. In zone C3 sample scores return to values observed in zone C1. Positive sample scores are driven by *Aulacoseira crassipunctata* and *Nitzschia palea*. Negative sample scores are driven by *Staurosira venter* and *Fragilaria brevistriata*.

PCA axis 2 is more strongly related to the diatom response to tephra deposition as there is a clear coherence between change in PCA axis 2 and the tephra deposition, specifically the responses of *Discostella pseudostelligera* and *Aulacoseira* taxa. Sample scores are weakly negative in zone C1, and become positive around the time of tephra deposition. In zone C2 sample scores are variable but positive then decrease towards the top of the zone, and increases in zone C3 where sample scores fluctuate again. Positive sample scores are dominated by *Aulacoseira lirata* and *Aulacoseira alpigena*. The negative sample scores are dominated by *Discostella pseudostelligera* and *Tabellaria flocculosa*.

For MLF PCA axis 1 accounts for 50.39% of the variance and represents the dominant gradient in the diatom data (Figure 6). PCA axis 2 accounts for only a further 8% of the variance. Sample scores of PCA axis 1 are strong and positive in zone F1, then become weakly negative in zone F2 around the time of Mazama tephra deposition. After tephra

deposition sample scores show a steady, increasing trend reverting to scores similar to those of the pre-tephra assemblage but not fully back to baseline conditions. Positive sample scores are driven by *Aulacoseira alpigena*, *Staurosira venter*, and *Aulacoseira lirata*. The negative sample scores are driven by *Brachysira brebissonii*, *Frustulia rhomboides*, *Craticula halophila* and *Navicula bremensis*.

### *Partial Redundancy Analysis*

For MLC partial RDA analyses (Table 3) revealed tephra to have a significant unique effect on the diatom assemblages in model 1, but not in models 2 and 3. Depth (directional change) had a significant unique effect in all analyses. LOI also had a significant unique effect except in MLC model 1 (Table 3).

For MLF the second model was applied to the dataset. In this model tephra was not significant, but depth and LOI had significant unique effects explaining 37.7% and 15.4% of the variance, respectively.

For MLC, the first model used an exponential decay rate of 0.8, assuming a 500 year recovery period with most recovery having happened within 200-250 years. This model reported tephra to have a significant unique effect on the diatom assemblage explaining 11.2% of the variance. Depth also had a significant unique effect explaining a further 10.6% of the variance. The second model used an exponential decay rate of 0.5, assuming a 200 year recovery period, with most recovery having happened within 100 years. In this model tephra was not significant but depth and LOI indicated significant unique effects explaining 12.7% and 9.1% of the variance, respectively. The third model assumes a recovery period of 80 years, with most recovery having happened within 20 years, through the application of a



decay rate of 0.1, and gave similar results to model 2 with tephra having no significant unique effect on the diatom assemblage but depth and LOI having a significant unique effect, explaining 12.6% and 11.3% of the variance, respectively (Table 3).

## DISCUSSION

Analysis of the diatoms from MLF and MLC clearly illustrates two very different assemblages, with a low proportion of planktonic taxa in MLF (Figure 6) compared to MLC (Figure 5) consistent with shallow and deeper lake water systems respectively at the time of the climactic eruption of Mount Mazama. The response to tephra deposition may therefore be expected to differ between the two locations. The species mix confirms that Moss Lake is an oligotrophic, low alkalinity system with high proportions of *Aulacoseira* taxa and *Brachysira brebissonii*, indicating sensitivity to impacts associated with acidification and/or changes in the nutrient status. The DCA gradients in both data sets for MLF and MLC had lengths of 1.1 and 0.7 SD units respectively, which suggests limited turn-over within the diatom assemblage (Lepš and Smilauer, 2014), however, changes are observed around the time of tephra deposition with MLC displaying a decline of *Discostella pseudostelligera*, and increases of *Aulacoseira* species, and MLF displaying notable decreases of *Aulacoseira* species and epiphytic taxa and increases of epipelagic taxa, in particular *Brachysira brebissonii*. The partial RDA analyses for MLF and model 2 and 3 for MLC revealed that tephra from Mount Mazama overall had no unique significant effect on the diatom assemblages. However, model 1 for MLC was the only model indicating a significant unique effect (11.2%) of tephra deposition independent of variation in depth or LOI. Importantly all of the other models for both MLF and MLC indicate that depth (directional change) had the most

significant unique effect on the diatom assemblage (MLF, 37.7%; MLC, 10.6-12.7%) with LOI also having a significant influence (MLF, 15.5%; MLC, 9.1-11.3%).

There is therefore evidence of a tephra effect from the diatom analyses, supported by model 1 of the partial RDA for MLC. However, the evidence for this tephra effect is not consistent between the two cores, or between the different models from MLC. Notably, the partial RDA shows that the underlying environmental changes (represented by depth and LOI) are more influential on the diatom assemblage than any tephra effects.

Nevertheless, there is evidence for a limited tephra effect and there are several hypotheses regarding the potential nature of tephra impacts on lake ecosystems, all of which have been reported in other tephra impact studies; 1) acidification in response to dry deposition of H<sub>2</sub>SO<sub>4</sub> following tephra deposition (Blinman *et al.*, 1979; Birks and Lotter, 1994; Bradbury *et al.*, 2004); 2) change in the nutrient status of the lake following tephra deposition (Barker *et al.*, 2003; Telford *et al.*, 2004); 3) habitat change following tephra deposition (Brant and Bahls, 1995; Telford *et al.*, 2004).

### **Tephra and acidification**

It is important to explore the acidification hypothesis, as this is one of the most commonly reported impacts of tephra deposition (Blinman *et al.*, 1979; Birks and Lotter, 1994; Bradbury *et al.*, 2004). In MLF (and to a lesser extent MLC) increases of *Brachysira brebissonii*, *Tabellaria flocculosa*, *Frustulia rhomboides* and *Eunotia naegelia* potentially support the acidification hypothesis as these are acid indicators (Anderson and Renberg, 1992; Fránková *et al.*, 2009) and the declines of the more acid sensitive *Fragilaria brevistriata* and *Staurosira*

427 *venter* are also consistent with an acidification (Anderson and Renberg, 1992). Importantly,  
428 however, the diatom response in MLF across all taxa is not consistent with acidification. For  
429 example, *Craticula halophila* increases significantly after tephra deposition and prefers  
430 alkaline conditions (Round *et al.*, 1990).

431 Similarly the diatom data from MLC could be interpreted as showing support for the  
432 acidification hypothesis due to the significance of model 1, and associated changes in  
433 *Fragilaria brevistriata* and *Staurosira venter* consistent with increased acidity following  
434 tephra deposition. However, the associated increases in *Nitzschia palea*, *Aulacoseira* species  
435 and *Discostella pseudostelligera* are counter to expected floristic trends following  
436 acidification, as they should decrease with increased acid loading (Anderson and Renberg,  
437 1992; Saros and Anderson, 2015). We therefore find no clear evidence of post-tephra  
438 acidification in this oligotrophic lake.

#### 440 **Tephra and nutrient status**

442 The increase of *Aulacoseira* taxa in MLC is consistent with a change in nutrient status, as  
443 *Aulacoseira* taxa thrive under silica rich conditions (Thwaites, 1848; Abella, 1988; Caballero  
444 *et al.*, 2006). The increase of silica at that time is most likely to be from tephra deposition,  
445 which also prevents the regeneration of nutrients such as phosphorus as it creates an  
446 impermeable barrier over the lakes sediment (Barker *et al.*, 2000; 2003). The reduction of  
447 phosphorous may have been a limiting factor for *Fragilaria brevistriata* and *Staurosira*  
448 *venter* (Abella, 1988), but their generally high tolerance suggests habitat change could have  
449 also been influential (discussed below). This hypothesis of a nutrient change is also supported

by the partial RDA analyses (Table 3) for MLC model 1, as *Aulacoseira crassipunctata* and other *Aulacoseira* taxa respond positively to tephra deposition, and thus the influx of silica. Likewise, *Fragilaria brevistriata* and *Staurosira venter* respond negatively in response to tephra in the partial RDA analyses, which might also suggest a habitat change (Table 3).

#### **Tephra and habitat change**

The floristic changes (increase of *Aulacoseira alpigena* and *Aulacoseira lirata*, decrease of *Fragilaria brevistriata* and *Staurosira venter* and increase of epipellic taxa) coincident with tephra deposition in MLC (and MLF despite the insignificance of tephra) may also suggest an alteration of habitat. The decrease of tychoplanktonic *Fragilaria brevistriata* and *Staurosira venter* and epiphytic taxa are indicative of disturbance and habitat change as aquatic plants are likely to be adversely affected by tephra deposition due to blanket burial. Although *Fragilaria brevistriata* and *Staurosira venter* are tychoplanktonic (Caballero *et al.*, 2006), they have been reported as epiphytic (Ehrlich, 1995; Stoermer *et al.*, 1996) due to their wide tolerances and tendency to attach themselves to benthic aquatic plants following a disturbance in the tychoplanktonic zone (e.g. tephra deposition). As such, these species often fluctuate along with aquatic vegetation (Caballero *et al.*, 2006). The local vegetation record from pollen analysis at Moss Lake (Egan *et al.*, 2016), summarised in Figure 7, shows a decrease of *Myriophyllum spicatum* and *Nuphar* due to blanket coverage inhibiting gas exchange and photosynthesis, which would result in a reduction in aquatic vegetation (submerged and emergent) thus epiphytic species and *Fragilaria brevistriata* and *Staurosira venter* would decline due to habitat loss (Telford *et al.*, 2004).

The increase of epipelagic taxa, *Staurosira lapidicola*, *Sellaphora pupula* and *Brachysira brebissonii* further demonstrates habitat change as these species increase in response to tephra deposition through colonisation of the newly deposited tephra (Telford *et al.*, 2004). The increase of *Aulacoseira* taxa also suggests habitat alteration as they can thrive in turbid waters with low light (Caballero *et al.*, 2006). Partial RDA confirmed tephra to be a significant variable in model 1, with *Staurosira venter* and *Fragilaria brevistriata* responding negatively to the tephra and the potential decline in suitable habitat as a result, and *Nitzschia palea* responding positively to the tephra due to the increase in habitat availability, further supporting this hypothesis.

### Impact summary

In summary, tephra from Mount Mazama had a significant unique effect on the diatom assemblage of the central core (MLC) according to partial RDA model 1, but no significant effect in the fringe core (MLF), or the central core (MLC) when applying partial RDA models 2 and 3. There is therefore some evidence of a tephra effect but this is inconsistent. We argue the nature of the effect is a change of habitat conditions and an increase in the Si:P ratio. These impacts lasted for 150-200 years (based on zone data, PCA axis 2 and the age depth model) to a maximum of 500 years with most recovery having happened within 200-250 years (based on partial RDA model one). The transition from diatom zone C2 to C3 reflects the point where the diatom assemblage reverts back to pre-tephra conditions, which is also evident from PCA axis 2 (Figure 5). This is demonstrated by increases of *Fragilaria brevistriata* and *Staurosira venter* to baseline levels, reflecting the 150-200 year recovery period. This recovery time period is nearly consistent with partial RDA model 1, which

implies a maximum recovery period of 500 years, but with most recovering happening within 200-250 years. Importantly all partial RDA models indicate that depth and LOI had significant unique effects. This suggests other drivers of change in the aquatic system at the time of the Mazama event, reflecting wider changes in climate, sedimentology and vegetation.

### **Alternative drivers of change**

All partial RDA analyses for MLC and MLF (Table 3) indicate that depth (surrogate for directional change) had the most significant unique effect on the diatom assemblage (MLF, 37.7%; MLC, 10.6-12.7%). LOI was also identified as an important variable (MLF, 15.5%; MLC, 9.1-11.3%). Taxa explained by depth in MLF are *Staurosira venter*, *Nitzschia palea*, *Brachysira brebissonii*, *Tabellaria flocculosa*, and *Aulacoseira lirata*. These taxa represent the most notable changes in the MLF diatom assemblage, and although the partial RDA analysis indicates depth to have the greatest significant unique effect there are a few caveats with the partial RDA analysis that must be highlighted. There is a potential issue with the MLF model as there was no evidence of recovery, which is what the model assumed. Given the sensitivity of lake fringes one might have expected a more pronounced impact of tephra here. Instead depth appears to be the significant variable but there is a possibility that depth could have been acting as a surrogate for tephra (as there is no evidence of recovery) and in fact tephra may be more important than indicated by this model. Despite this, all but one model for MLC indicate an insignificant independent response to tephra deposition, with depth (directional change) being the main driver.

521 Taxa explained by depth in MLC are *Aulacoseira crassipunctata* and *Aulacoseira lirata* in all  
522 models and *Discostella pseudostelligera* in model one (Table 3). *Discostella pseudostelligera*  
523 are likely to be responding to ongoing climate change as PCA axis 1 (Figure 5) is  
524 representative of short term environmental change and correlates well with variations in  
525 *Discostella pseudostelligera*. Further, Egan (2016) report fluctuations of *Aulacoseira* taxa  
526 and *Discostella pseudostelligera* in response to climatic changes at that time. LOI also had a  
527 significant unique effect and is likely to reflect the change in sedimentology around the time  
528 of Mazama tephra deposition from silty gyttja to organic peaty silt (Figure 2). This change in  
529 sedimentology could potentially be as a result of tephra deposition as it can reduce infiltration  
530 and increase surface wetness potentially creating waterlogged conditions for peaty silt to  
531 develop, however, as models 2 and 3 for MLC and MLF indicate an insignificant effect of  
532 tephra, this is unlikely. Alternatively, LOI could be influenced by longer-term environmental  
533 change. During the time of tephra deposition Moss Lake was in a period of transition with an  
534 increase of nutrients from both a warmer climate (beginning 8000 cal yr BP until 6500 cal yr  
535 BP) and the developing conifer forest ecosystem, particularly *Pseudotsuga menziesii*, *Tsuga*  
536 *heterophylla* and Cupressaceae, at that time (Egan *et al.*, 2016), summarised in Figure 7b.  
537 There is also evidence that during the Holocene the lake was undergoing hydrosere  
538 succession in the marginal areas of the lake basin as evidenced by the increasing LOI and  
539 development of silty peats (Figure 6). These catchment wide changes allowed longer growing  
540 seasons, increased nutrient availability and increased habitat availability for diatoms,  
541 increasing diatom diversity (Egan, 2016). Thus the addition of tephra may have amplified  
542 these changes in nutrient status and hydrosere succession as the addition of silica into the  
543 system would have a positive effect on some diatoms (i.e. *Aulacoseira* taxa), while the tephra  
544 itself further increases habitat availability for the epipelagic species and contributes to sediment

influx. However, given that the partial RDA analyses only indicate that tephra had a significant unique effect in one model it can be concluded that the effect of tephra on the aquatic system of Moss Lake was minimal in relation to underlying environmental trends.

## CONCLUSION

The climactic eruption of Mount Mazama was a major volcanic event in North America during the Holocene. At Moss Lake up to 50 mm of tephra was deposited. There is some evidence for significant, and independent impacts of this tephra on the aquatic ecosystem, but these are not consistent between the central and fringe core locations. Partial RDA analyses indicated that tephra had no unique significant effect on the diatom assemblages of the fringe core location, whereas the partial RDA models for the central core location based on a 500 year maximum recovery period, with most recovery happening with 200-250 years, were significant.

The diatom response recorded in both the shallow and deep water lake systems suggests that there was a change in habitat availability with a reduction in tychoplanktonic taxa (particularly *Fragilaria brevistriata* and *Staurosira venter*) and epiphytic taxa, and an increase in epipelagic taxa (particularly *Brachysira brebissonii* and *Frustulia rhomboides*). There was also a change in the Si:P ratio with an increase of *Aulacoseira* taxa recorded in the deep water lake system. These changes are coincident with the timing of tephra deposition and are also associated with ongoing environmental change within the catchment, with both a warmer climate and the expansion of a conifer forest evidenced by pollen analyses on MLF and MLC. The climate and catchment wide changes could have been amplified by tephra



deposition due to the addition of silica contributing to nutrient availability and the sediment (tephra) influx increasing epipelagic habitat availability.

Overall the partial RDA analyses indicate some evidence of an effect, likely to be habitat change, but this is not consistent between the central and fringe core and the tephra impact is not as important as changes in the assemblages caused by underlying environmental trends. There is a natural tendency to equate any coincidental diatom change with the impact of tephra deposition. Without high resolution analyses, cross correlations with multiple cores and other records, and robust statistical analyses, it is difficult to determine how influential tephra is.

## ACKNOWLEDGEMENTS

This work was supported by the NERC Radiocarbon Facility NRCF010001 (allocation numbers 1877.1014; 1728.1013). Fieldwork was partially funded by the Royal Geographical Society with IBG (Geographical Club Award Ref. 03.13). We thank Danielle Alderson (The University of Manchester), Douglas H. Clark and Harold N. Wershow (Western Washington University) for assistance in the field.

## SUPPLEMENTARY AND ARCHIVED DATA

All diatom and stratigraphic data are available from:  
<https://doi.pangaea.de/10.1594/PANGAEA.890666> in addition to the supplementary data  
already discussed within the manuscript.

## REFERENCES

- Abella, S.E., 1988. The effect of Mt. Mazama ashfall on the planktonic diatom community of Lake Washington. *Limnology and oceanography*, 33, 1376–1385.
- Anderson, N.J., Renberg, I., 1992. A palaeolimnological assessment of diatom production responses to lake acidification. *Environmental Pollution*, 78, 113–119.
- Ayris, P.M., Delmelle, P., 2012. The immediate environmental effects of tephra emission. *Bulletin of Volcanology*, 74, 1905–1936.
- Barker, P., Telford, R., Merdaci, O., Williamson, D., Taieb, M., Vincens, A., Gibert, E., 2000. The sensitivity of a Tanzanian crater lake to catastrophic tephra input and four millennia of climate change. *The Holocene*, 10, 303–310.
- Barker, P., Williamson, D., Gasse, F., Gibert, E., 2003. Climatic and volcanic forcing revealed in a 50,000-year diatom record from Lake Massoko, Tanzania. *Quaternary Research*, 60, 368–376.
- Battarbee, R.W., 1986. Diatom analysis. In: Berglund, B.E. (Ed.), *Handbook of Holocene Palaeoecology and Palaeohydrology*. John Wiley & Sons LTD, Chichester, pp. 527–570.
- Battarbee, R., Kneen, M.J., 1982. The use of electronically counted microspheres in absolute diatom analysis. *Limnology and oceanography*, 27, 184–188.

610 Bennett, K.D., 1996. Determination of the number of zones in a biostratigraphical sequence.  
611 *New Phytologist*, 132, 155–170.

612 Bennett, K.D., 2007. Psimpoll and Pscomb programs for plotting and analysis [Online].  
613 Available from: <http://www.chrono.qub.ac.uk/psimpoll/psimpoll.html> (accessed 2.18.15).

614 Birks, H.J.B., Lotter, A.F., 1994. The impact of the Laacher See Volcano (11 000 yr B.P.) on  
615 terrestrial vegetation and diatoms. *Journal of Paleolimnology*, 11, 313–322.

616 Blackford, J.J., Payne, R.J., Heggen, M.P., de la Riva Caballero, A., van der Plicht, J., 2014.  
617 Age and impacts of the caldera-forming Aniakchak II eruption in western Alaska.  
618 *Quaternary Research*, 82, 85–95.

619 Blinman, E., Mehringer, P.J., Sheppard, J.C., 1979. Pollen influx and the deposition of  
620 Mazama and Glacier Peak tephra. In: Sheets, P., Grayson, D., (Eds.), *Volcanic Activity and*  
621 *Human Ecology*. Academic Press Inc, London, pp. 393–425.

622 ter Braak, C., Prentice, I., 1988. *A theory of gradient analysis*. Academic Press Inc, London.

623 ter Braak, C., Šmilauer, P., 2012. *Canoco reference manual and user's guide: software for*  
624 *ordination, version 5.0*. Microcomputer Power, Ithaca: USA.

625 Bradbury, P.J., Colman, S.M., Dean, W.E., 2004. Limnological and Climatic Environments at  
626 Upper Klamath Lake, Oregon during the past 45 000 years. *Journal of Paleolimnology*, 31,  
627 167–188.

628 Bronk Ramsey, C., 2014. OxCal V. 4.2 [Online]. Available from:  
629 <https://c14.arch.ox.ac.uk/oxcal/OxCalhtml> (accessed 11.20.14).

630 Brant, L., Bahls, L., 1995. Paleoenvironmental impacts of volcanic eruptions upon a diatom  
631 community. In: J. P. Kociolek and M. J. Sullivan (eds), *A century of diatom research in*

632 *North America: a tribute to the distinguished careers of Charles W. Reimer and Ruth Patrick.*  
633 Koeltz Scientific: Stuttgart.

634 Caballero, M., Vázquez, G., Lozano-García, S., Rodríguez, A., Sosa-Nájera, S., Ruiz-  
635 Fernández, A.C. and Ortega, B., 2006. Present limnological conditions and recent (ca. 340 yr)  
636 palaeolimnology of a tropical lake in the Sierra de Los Tuxtlas, Eastern Mexico. *Journal of*  
637 *Paleolimnology*, 35(1), pp.83-97.

638 Colman, S.M., Bradbury, J., McGeehin, J.P., Holmes, C.W., Edginton, D., Sarna-Wojcicki,  
639 A.M., 2004. Chronology of Sediment Deposition in Upper Klamath Lake, Oregon. *Journal of*  
640 *Paleolimnology*, 31, 139–149.

641 Dragovich, J.D., Logan, R.L., Schasses, H.W., Walsh, T.J., Lingley, W.S.J., Norman, D.K.,  
642 Gerstel, W.J., Lapen, T.J., Schuster, J.E., Meyers, K.D., 2002. Geological map of  
643 Washington- Northwest Quadrant: Washington Division of Geology and Earth Resources  
644 Geological Map GM-50, 3 sheets, scale 1:250,000.

645 Egan, J., 2016. *Impact and significance of tephra deposition from Mount Mazama and*  
646 *Holocene climate variability in the Pacific Northwest USA*. Thesis: The University of  
647 Manchester.

648 Egan, J., Fletcher, W.J., Allott, T.E.H., Lane, C.S., Blackford, J.J., Clark, D.H., 2016. The  
649 impact and significance of tephra deposition on a Holocene forest environment in the North  
650 Cascades, Washington, USA. *Quaternary Science Reviews*, 137, 135–155.

651 Egan, J., Staff, R.A., Blackford, J., 2015. A revised age estimate of the Holocene Plinian  
652 eruption of Mount Mazama, Oregon using Bayesian statistical modelling. *The Holocene*, 25,  
653 1054–1067.

654 Ehrlich, A., 1995. *Atlas of the Inland-water Diatom Flora of Israel*. The Geological Survey  
 655 of Israel and the Israel Academy of Sciences and Humanities, Jerusalem, 166 pp. + 60 plates.

656 Fránková, M., Bojková, J., Pouličková, A., Hájek, M., 2009. The structure and species  
 657 richness of the diatom assemblages of the Western Carpathian spring fens along the gradient  
 658 of mineral richness. *Fottea*, 9, 355–368.

659 Heinrichs, M.L., Walker, I.R., Mathewes, R.W., Hebda, R.J. 1999. Holocene chironomid-  
 660 inferred salinity and paleovegetation reconstruction from Kilpoola Lake, British Columbia.  
 661 *Géographie physique et Quaternaire*, 53, 211–221.

662 Hickman, M., Reasoner, M.A., 1994. Diatom responses to late Quaternary vegetation and  
 663 climate change, and to deposition of two tephras in an alpine and a sub-alpine lake in Yoho  
 664 National Park, British Columbia. *Journal of Paleolimnology*, 11, 173–188.

665 Hill, M., Gauch, H., 1980. Detrended correspondence analysis: an improved ordination  
 666 technique. *Vegetatio*, 42, 47–58.

667 Kelly, M.G., Bennion, H., Cox, E.J., Goldsmith, B., Jamieson, J., Juggins, S., Mann, D.G.,  
 668 Telford, R.J., 2005. Craticula [Online]. Common freshwater diatoms of Britain and Ireland:  
 669 an interactive key. Environment Agency, Bristol. Available from:  
 670 <http://craticula.ncl.ac.uk/EADiatomKey/html/index.html> (accessed 11.10.15).

671 Krammer, K., Lange-Bertalot, H., 1991. *Süßwasserflora von Mitteleuropa vol 2/4*  
 672 *Bacillariophyceae*. Gustav Fischer Verlag, Stuttgart.

673 Krammer, K., Lange-Bertalot, H., 1999a. *Süßwasserflora von Mitteleuropa vol 2/1*  
 674 *Bacillariophyceae*. Spektrum Akademischer verlag GmbH, Berlin.

675 Krammer, K., Lange-Bertalot, H., 1999b. *Süßwasserflora von Mitteleuropa vol 2/2*  
676 *Bacillariophyceae*. Spektrum Akademischer verlag GmbH, Berlin.

677 Lallement, M., Macchi, P.J., Vigliano, P., Juarez, S., Rechencq, M., Baker, M., Bouwes, N.,  
678 Crawl, T., 2016. Rising from the ashes: Changes in salmonid fish assemblages after  
679 30months of the Puyehue-Cordon Caulle volcanic eruption. *The Science of the total*  
680 *environment*, 541, 1041–51.

681 Lepš, J., Smilauer, P., 2014. *Multivariate analysis of ecological data using CANOCO 5*, 2nd  
682 ed. Cambridge University Press, Cambridge.

683 Lotter, A.F., Anderson, N.J., 2012. Limnological Responses to Enbironmental Changes at  
684 Inter-annual to Decadal Time-scales. In: Birks, H.J.B., Lotter, A.F., Juggins, S., Smol, J.P.,  
685 (Eds.), *Tracking Environmental Change Using Lake Sediments, Developments in*  
686 *Paleoenvironmental Research 5*. Springer, New York, pp. 557–578.

687 Lotter, A.F., Birks, H., 1993. The Impact Of The Laacher See Tephra On Terrestrial And  
688 Aquatic Ecosystems In The Black-Forest, Southern Germany. *Journal of Quaternary*  
689 *Science*, 8, 263–276.

690 Mass, C.F., Portman, D.A., 1989. Major Volcanic Eruptions and Climate: A Critical  
691 Evaluation. *Journal of Climate*, 2, 566–593.

692 McCormick, M.P., Thomason, L.W., Trepte, C.R., 1995. Atmospheric effects of the Mt  
693 Pinatubo eruption. *Nature*, 373, 399–404.

694 Orloci, L., 1966. Geometric Models in Ecology: I. The Theory and Application of Some  
695 Ordination Methods. *Journal of Ecology*, 54, 193–215.

696 Payne, R., Blackford, J., 2008. Distal volcanic impacts on peatlands: palaeoecological  
697 evidence from Alaska. *Quaternary Science Reviews*, 27, 2012–2030.

698 Payne, R.J. and Egan, J., 2017. Using palaeoecological techniques to understand the impacts  
699 of past volcanic eruptions. *Quaternary International*. In press, pp.1-12.

700 Porter, S.C., Swanson, T.W., 1998. Radiocarbon age constraints on rates of advance and  
701 retreat of the Puget Lobe of the Cordilleran Ice Sheet during the last glaciation. *Quaternary*  
702 *Research*, 50, 205-213.

703 Power, M.J., Whitlock, C. & Bartlein, P.J., 2011. Postglacial fire, vegetation, and climate  
704 history across an elevational gradient in the Northern Rocky Mountains, USA and Canada.  
705 *Quaternary Science Reviews*, 30(19-20), 2520–2533.

706 Pyne-O'Donnell, S.D., Hughes, P.D., Froese, D.G., Jensen, B.J., Kuehn, S.C., Mallon, G.,  
707 Amesbury, M.J., Charman, D.J., Daley, T.J., Loader, N.J. and Mauquoy, D., 2012. High-  
708 precision ultra-distal Holocene tephrochronology in North America. *Quaternary Science*  
709 *Reviews*, 52, 6–11.

710 Rao, C., 1964. The use and interpretation of principal component analysis in applied research.  
711 *Sankhyā: The Indian Journal of Statistics, Series A*, 26, 329–358.

712 Reimer, P., Bard, E., Bayliss, A., Beck, J.W., Blackwell, P.G., Bronk Ramsey, C., Buck,  
713 C.E., Cheng, H., Edwards, R.L., Friedrich, M., Grootes, P.M., Guilderson, T.P., Haflidason,  
714 H., Hajdas, I., Hatte, C., Heaton, T.J., Hoffman, D.L., Hogg, A.G., Hughen, K.A., Kaiser,  
715 K.F., Kromer, B., Manning, S.W., Niu, M., Reimer, R.W., Richards, D.A., Scott, E.M.,  
716 Southon, J.R., Staff, R.A., Turney, C.S.M., van der Plicht, J., 2013. IntCal13 and Marine13  
717 Radiocarbon Age Calibration Curves 0–50,000 Years cal BP. *Radiocarbon*, 55, 1869–1887.

718 Renberg, I., 1990. A procedure for preparing large sets of diatom slides from sediment cores.  
 719 *Journal of Paleolimnology*, 4, 87-90.

720 Rose, W.I., Durant, A.J., 2009. Fine ash content of explosive eruptions. *Journal of*  
 721 *Volcanology and Geothermal Research*, 186, 32–39.

722 Round, F., Crawford, R., Mann, D., 1990. *The diatoms: biology & morphology of the genera*.  
 723 Cambridge University Press: Cambridge.

724 Saros, J.E., Anderson, N.J., 2015. The ecology of the planktonic diatom *Cyclotella* and its  
 725 implications for global environmental change studies. *Biological reviews of the Cambridge*  
 726 *Philosophical Society*, 90, 522–41.

727 Spaulding, S., 2014. Diatoms of the United States [Online]. Available from:  
 728 <http://westerndiatoms.colorado.edu/> (accessed 10.31.14).

729 Staff, R.A., Bronk Ramsey, C., Bryant, C.L., Brock, F., Payne, R.L., Schlolaut, G., Marshall,  
 730 M.H., Brauer, A., Lamb, H.F., Tarasov, P., Yokoyama, Y., Haraguchi, T., Gotanda, K.,  
 731 Yonenobu, H., Nakagawa, T., 2011. New <sup>14</sup>C Determinations from Lake Suigetsu, Japan:  
 732 12,000 to 0 cal BP. *Radiocarbon*, 53, 511–528.

733 Stoermer, E.F., Emmert G., Julius M.L. and Schelske C.L. 1996. Paleolimnologic evidence of  
 734 rapid recent change in Lake Erie's trophic status. *Canadian Journal of Fisheries and Aquatic*  
 735 *Sciences*, 53: 1451–1458

736 Stoffel, M., Khodri, M., Corona, C., Guillet, S., Poulain, V., Bekki, S., Guiot, J., Luckman,  
 737 B.H., Oppenheimer, C., Lebas, N., Beniston, M., Masson-Delmotte, V., 2015. Estimates of  
 738 volcanic-induced cooling in the Northern Hemisphere over the past 1,500 years. *Nature*  
 739 *Geoscience*, 8, 784-788.



Stone, J.R., 2005. *A High-Resolution Record Of Holocene Drought Variability And The Diatom Stratigraphy Of Foy Lake, Montana*. Thesis: University of Nebraska.

Telford, R., Barker, P., Metcalfe, S., Newton, A., 2004. Lacustrine responses to tephra deposition: examples from Mexico. *Quaternary Science Reviews*, 23, 2337–2353.

Thwaites, G.H.K., 1848. XVI.— Further observations on the Diatomaceæ; with descriptions of new genera and species. *Journal of Natural History Series 2*, 1, 161–172.

Zdanowicz, C.M., Zielinski, G.A., Germani, M.S., 1999. Mount Mazama eruption: Calendrical age verified and atmospheric impact assessed. *Geology*, 27, 621–624.

Zielinski, G.A., 2000. Use of paleo-records in determining variability within the volcanism–climate system. *Quaternary Science Reviews*, 19, 417–438.

Table 1: Conventional ( $^{14}\text{C}$  yr BP), calibrated (cal yr BP) and modelled (at 95.4% probability range) radiocarbon ages for MLC previously reported in Egan *et al.*, (2016).

Lab no.	Depth (cm)	Material	Age ( $^{14}\text{C}$ years BP $\pm$ 1 SD)	Age range (cal yr BP 2 SD)	Modelled age range (cal yr BP 95.4% probability range)
<b>SUERC-59476</b>	305	Organic sediment	6330 $\pm$ 36	7410-7167	7286-7163
<b>SUERC-59477</b>	315	Organic sediment	6590 $\pm$ 38	7565-7430	7486-7424
<b>SUERC-59478</b>	321	Organic sediment directly above Mazama	6687 $\pm$ 39	7619-7480	7622-7531
<b>Mazama*</b>	324	-	-	7682-7584*	
<b>SUERC-59479</b>	345	Organic sediment	7430 $\pm$ 39	8344-8180	8351-8178

\*Age range from Egan et al. (2015)

\*\* Age range based on deposition model

755 Table 2: Summary of the diatom assemblage from MLC and MLF, and their associated  
756 zones.

Zone	Depth (cm)	Diatom description	Diatom concentration
MLC			
C3	316.5	<ul style="list-style-type: none"> <li>- <i>Discotella pseudostelligera</i> decrease to 50% but remain dominant.</li> <li>- Tycho planktonic species dominate the benthic community (up to 50%).</li> </ul>	Variable ( $2 \times 10^8$ - $10 \times 10^7$ per g dry weight).
C2	325	<ul style="list-style-type: none"> <li>- Planktonic and tycho planktonic species continue to dominate (90%).</li> <li>- <i>Aulacoseira crassipunctata</i> appear in greater abundance (10%).</li> <li>- <i>Fragilaria brevistriata</i> and <i>Staurosira venter</i> start to increase from 5% to 20%.</li> <li>- Epipelagic species <i>Nitzschia palea</i>, <i>Navicula bremensis</i> and <i>Sellaphora pupula</i> briefly increase.</li> </ul>	Variable ( $1 \times 10^8$ - $13 \times 10^7$ per g dry weight).
C1	340	<ul style="list-style-type: none"> <li>- Planktonic <i>Discotella pseudostelligera</i> dominate (up to 60%).</li> <li>- Upon tephra deposition tycho planktonic <i>Aulacoseira</i> species increase but <i>Fragilaria brevistriata</i> and <i>Staurosira venter</i> decrease.</li> </ul>	Increases upon tephra deposition.
MLF			
F2	156.8	<ul style="list-style-type: none"> <li>- Epipelagic species become increasingly important, especially <i>Brachysira brebissonii</i>, <i>Craticula halophila</i> and <i>Nitzschia palea</i>, which increase during tephra deposition</li> <li>- Epiphytic species modestly decline following tephra deposition.</li> <li>- Tycho planktonic species decrease after tephra deposition, <i>Staurosira venter</i> nearly disappears.</li> </ul>	Low with a maximum of $1 \times 10^8$ per g dry weight.

F1	160	-	Tychoplanktonic species fluctuate from 10% to 50% decreasing just before tephra deposition.	Variable (0.5x10 <sup>8</sup> - 7x10 <sup>8</sup>
		-	Epiphytic species dominate just before and upon tephra deposition (~40%).	per g dry weight).
		-	<i>Discotella pseudostelligera</i> briefly appears before tephra deposition and declines towards the top of the zone.	
		-	<i>Tabellaria flocculosa</i> increases just before tephra deposition, then declines.	

Table 3: Results of partial redundancy analysis of the diatom stratigraphical data sets of Moss Lake central and Moss Lake fringe reporting the unique effects and their significance. Those in **bold** are significant. Diatom species with an abundance of >5% or present in at least 10 samples was used in the analysis. Lower down on the table is the percentage variation of the diatoms, which indicates which species are most influenced by the variables. The +/- signs means the species had either a positive or negative relationship with that particular variable.

Variable	Tephra	Depth	LOI
Co-variables	Depth + LOI	Tephra + LOI	Tephra + Depth
Moss Lake Fringe (MLF)			
Unique effect (%)	3.6	37.7	15.4
Significance of unique effect	0.204	0.01	0.031
Moss Lake Central (MLC)- Model 1			
Unique effect (%)	11.2	10.6	6.1
Significance of unique effect	0.02	0.02	0.103
Moss Lake Central (MLC)- Model 2			
Unique effect (%)	7.1	12.7	9.1
Significance of unique effect	0.059	0.037	0.048
Moss Lake Central (MLC)- Model 3			
Unique effect (%)	4.5	12.6	11.3
Significance of unique effect	0.252	0.046	0.031
% Variation of Response Variable (Diatoms)			
Tephra	Depth	LOI	
Moss Lake Fringe			
<i>Eunotia obliquistriata</i> (+7.8), <i>Eunotia macroglossa</i> (-7.8), <i>Stauroneis lapidicola</i> (-7.5), <i>Eunotia arcus</i> (+6.6), <i>Navicula bremensis</i> (-5.1)	<i>Staurosira venter</i> (+56.2), <i>Nitzschia palea</i> (-55.2), <i>Brachysira brebissonii</i> (-50.2), <i>Tabellaria flocculosa</i> (-47.0), <i>Aulacoseira lirata</i> (+42.6)	<i>Aulacoseira alpigena</i> (+23.1), <i>Brachysira brebissonii</i> (-18.5), <i>Gomphonema gracile</i> (+17.5), <i>Frustulia rhomboides</i> (-17.0), <i>Stauroneis kreigeri</i> (+13.6)	
Moss Lake Central- Model 1			
<i>Staurosira venter</i> (-65.3), <i>Fragilaria brevistriata</i> (-47.5), <i>Aulacoseira crassipunctata</i> (+44.9), <i>Nitzschia palea</i> (+36.0), <i>Discostella pseudostelligera</i> (+31.1)	<i>Aulacoseira crassipunctata</i> (-29.8), <i>Aulacoseira lirata</i> (-15.3), <i>Discostella pseudostelligera</i> (+15.2), <i>Aulacoseira alpigena</i> (-7.8)	<i>Aulacoseira crassipunctata</i> (-13.2), <i>Aulacoseira granulata</i> (-12.2), <i>Staurosira venter</i> (+6.5)	
Moss Lake Central- Model 2			
<i>Staurosira venter</i> (-55.8), <i>Aulacoseira crassipunctata</i> (+42.5), <i>Fragilaria brevistriata</i> (-41.6), <i>Aulacoseira valida</i> (+24.5), <i>Nitzschia palea</i> (+23.8)	<i>Aulacoseira crassipunctata</i> (-38.4), <i>Aulacoseira lirata</i> (-19.2), <i>Pseudostaurosira elliptica</i> (+10.0), <i>Staurosira venter</i> (+9.6)	<i>Aulacoseira crassipunctata</i> (-19.8), <i>Staurosira venter</i> (+16.7), <i>Fragilaria brevistriata</i> (+11.8), <i>Aulacoseira granulata</i> (-9.4)	
Moss Lake Central- Model 3			
<i>Aulacoseira valida</i> (+19.0), <i>Staurosira venter</i> (-17.4), <i>Fragilaria brevistriata</i> (-9.0)	<i>Aulacoseira crassipunctata</i> (-38.0), <i>Aulacoseira lirata</i> (-18.5), <i>Staurosira venter</i> (+12.0), <i>Pseudostaurosira elliptica</i> (+10.6)	<i>Staurosira venter</i> (+26.9), <i>Aulacoseira crassipunctata</i> (-21.7), <i>Fragilaria brevistriata</i> (+19.1), <i>Aulacoseira pusilla</i> (-10.4), <i>Aulacoseira granulata</i> (-10.1)	

FIGURES

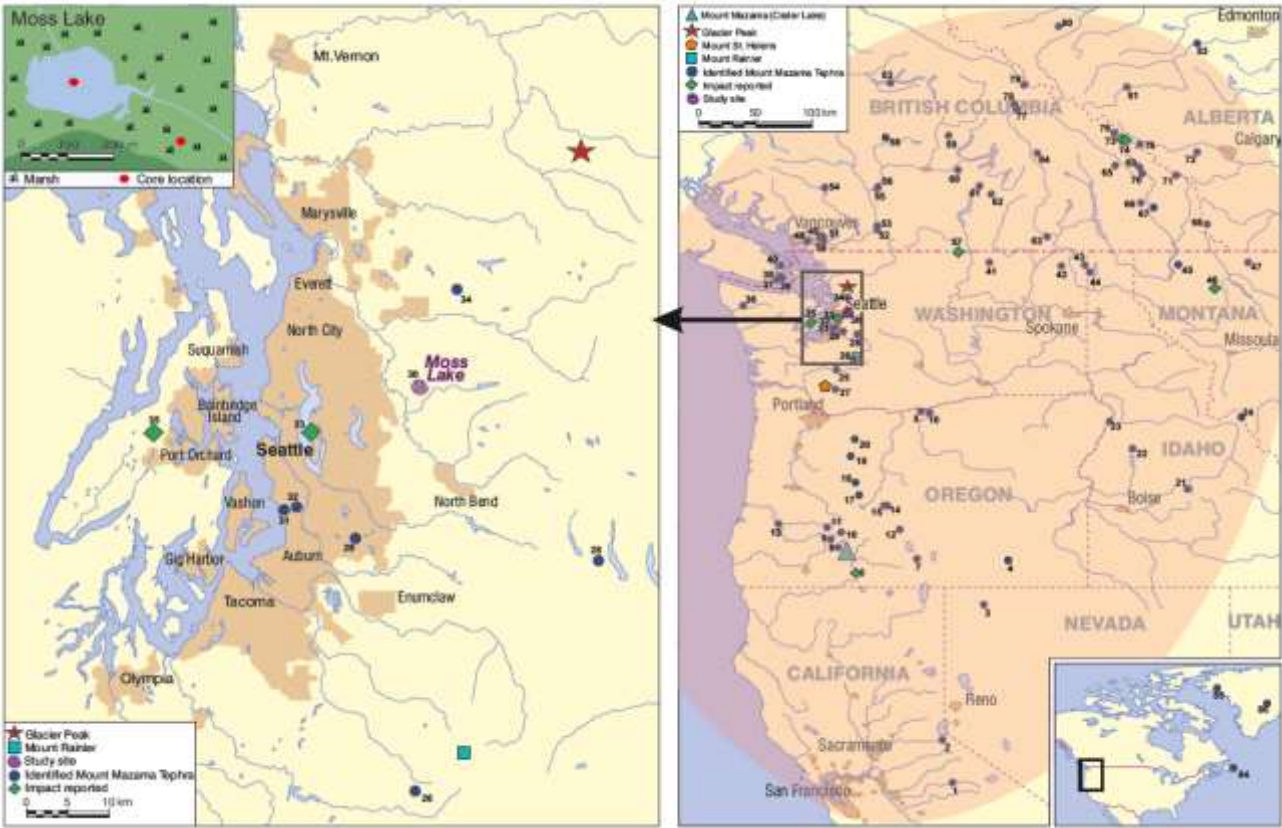


Figure 1: Extent of deposition from the Plinian eruption of Mount Mazama, and sites where it has previously been identified. The elliptical shaded envelope in the map to the right shows the extent of recorded visible Mount Mazama tephra deposition. True tephra dispersal was much greater with cryptotephra having been found as far as Newfoundland (Pyne-O'Donnell et al., 2012) and Greenland (Zdanowicz et al., 1999). The locations of Moss Lake, Mount Mazama and Glacier Peak are also highlighted. The shading around cities indicates the size and distribution of major urban areas. A key is provided for the numbered sites in supplementary material Table 2.

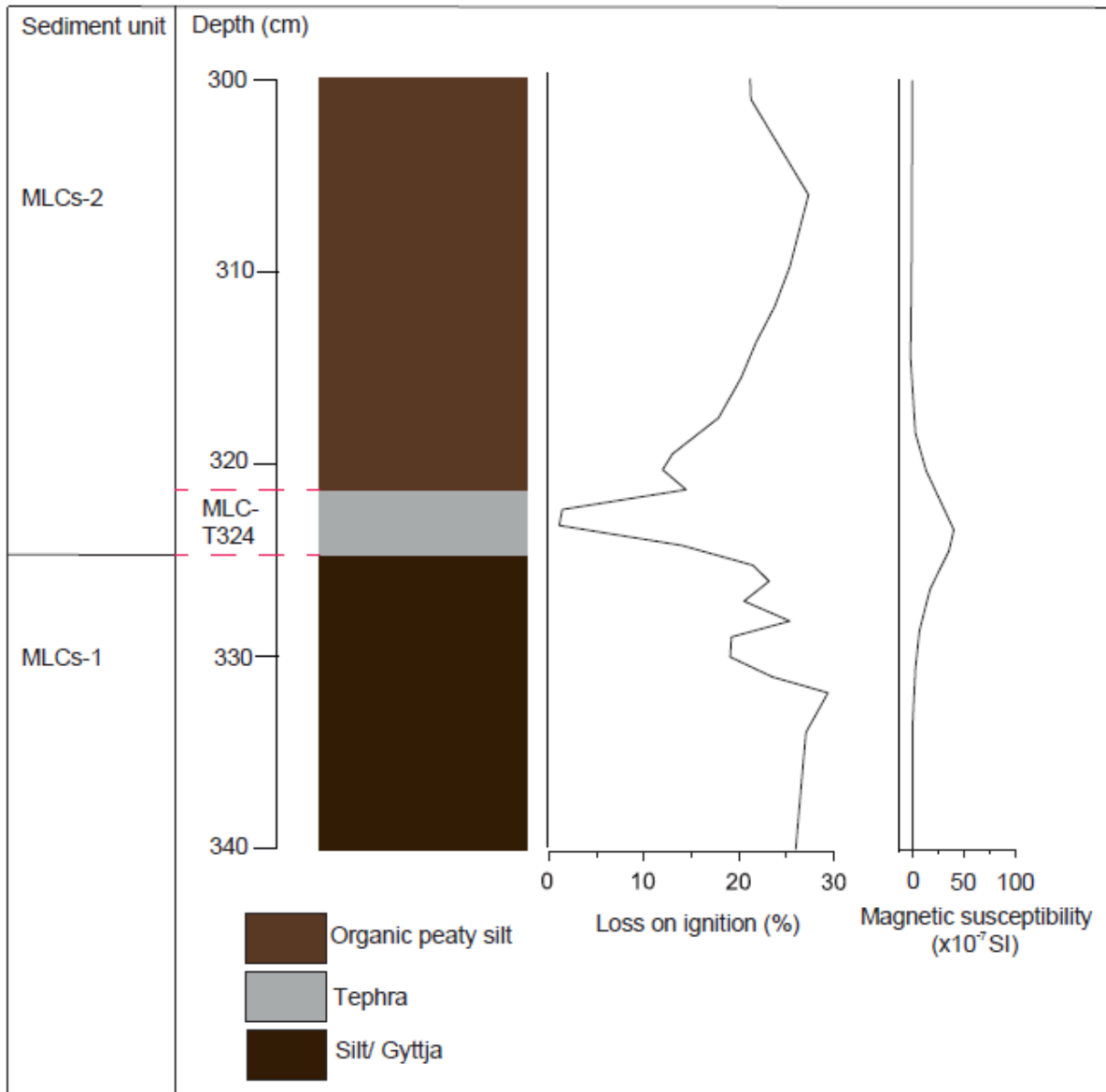
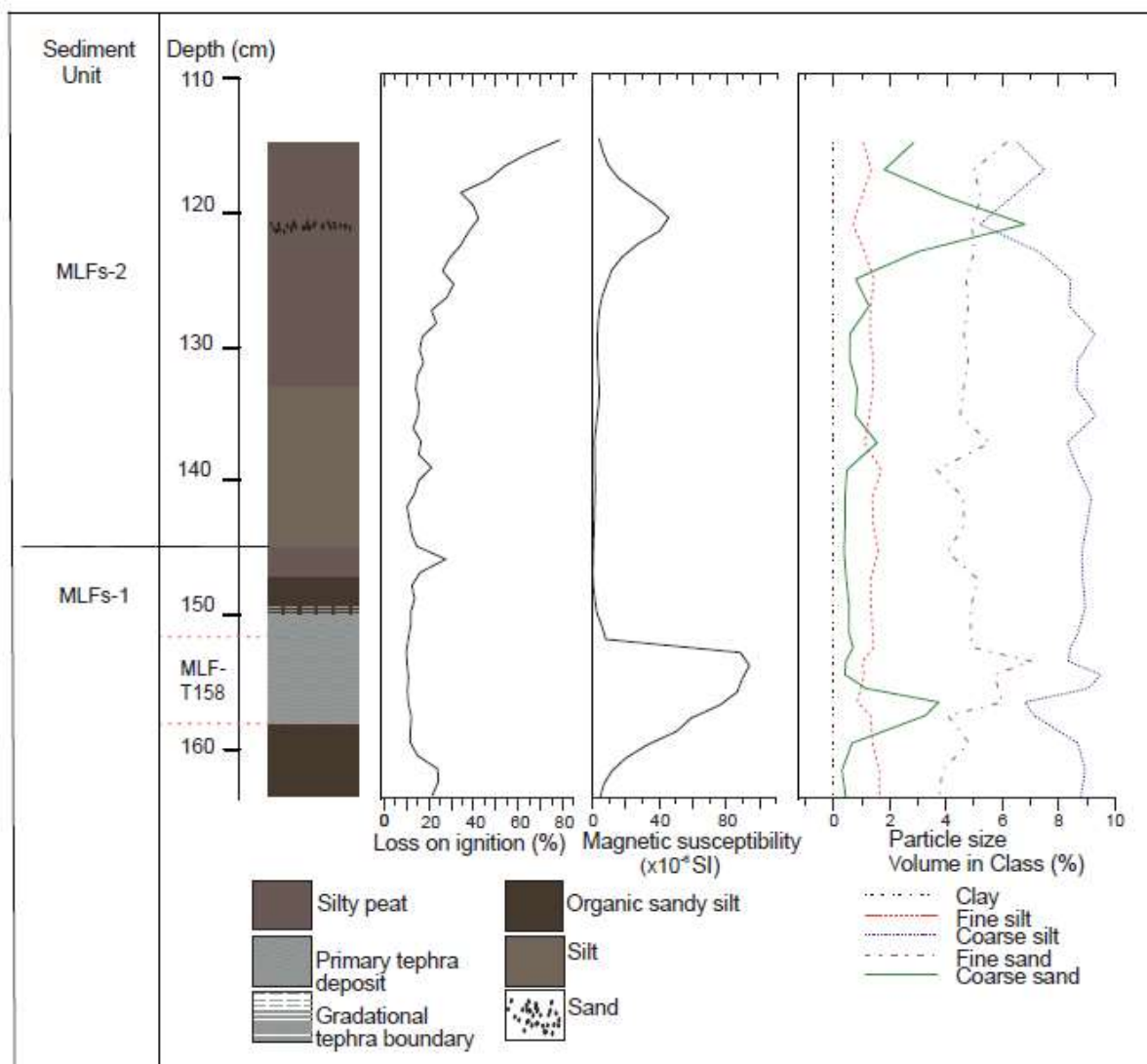


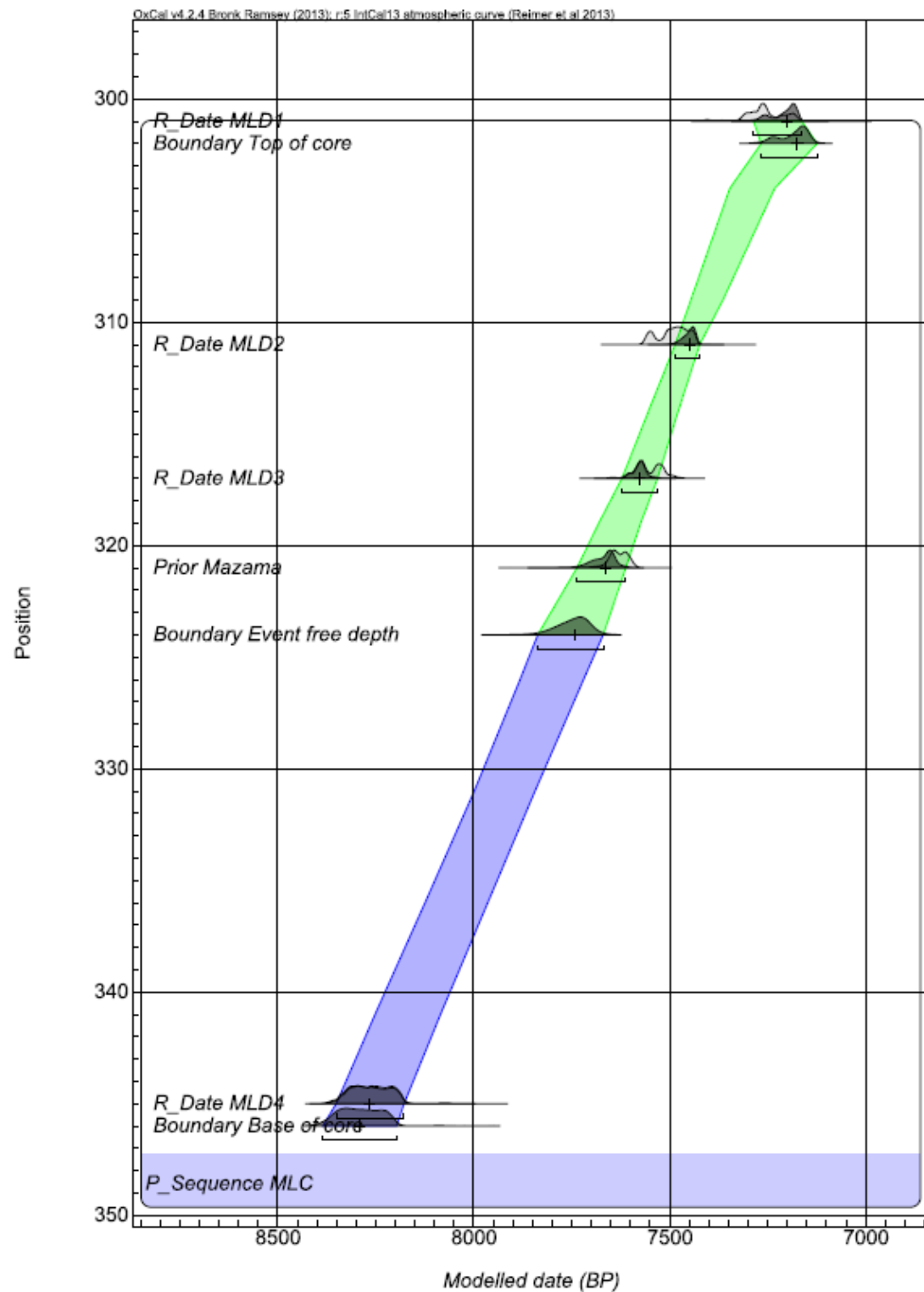
Figure 2: Lithology, % LOI, magnetic susceptibility and carbonate content of MLC.



783

784 Figure 3: Lithology, % LOI, magnetic susceptibility, carbonate content and particle size of

785 MLF



786

787 Figure 4: Bayesian age-depth (OxCal v.4.2 (Bronk Ramsey, 2014)) model for MLC derived

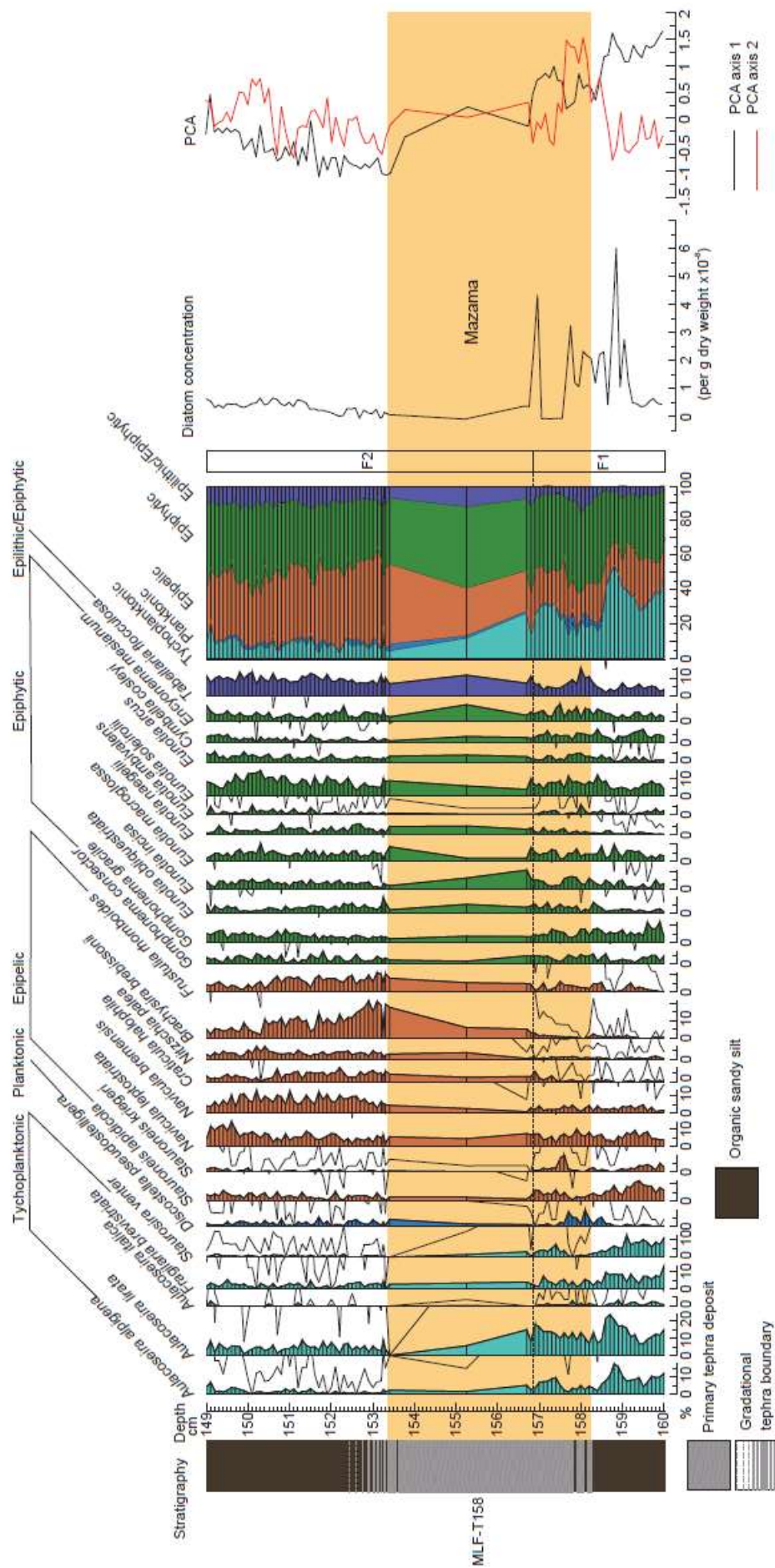
788 from the comparison of the radiocarbon ages calibrated using the IntCal13 (Reimer, 2013)

789 dataset.



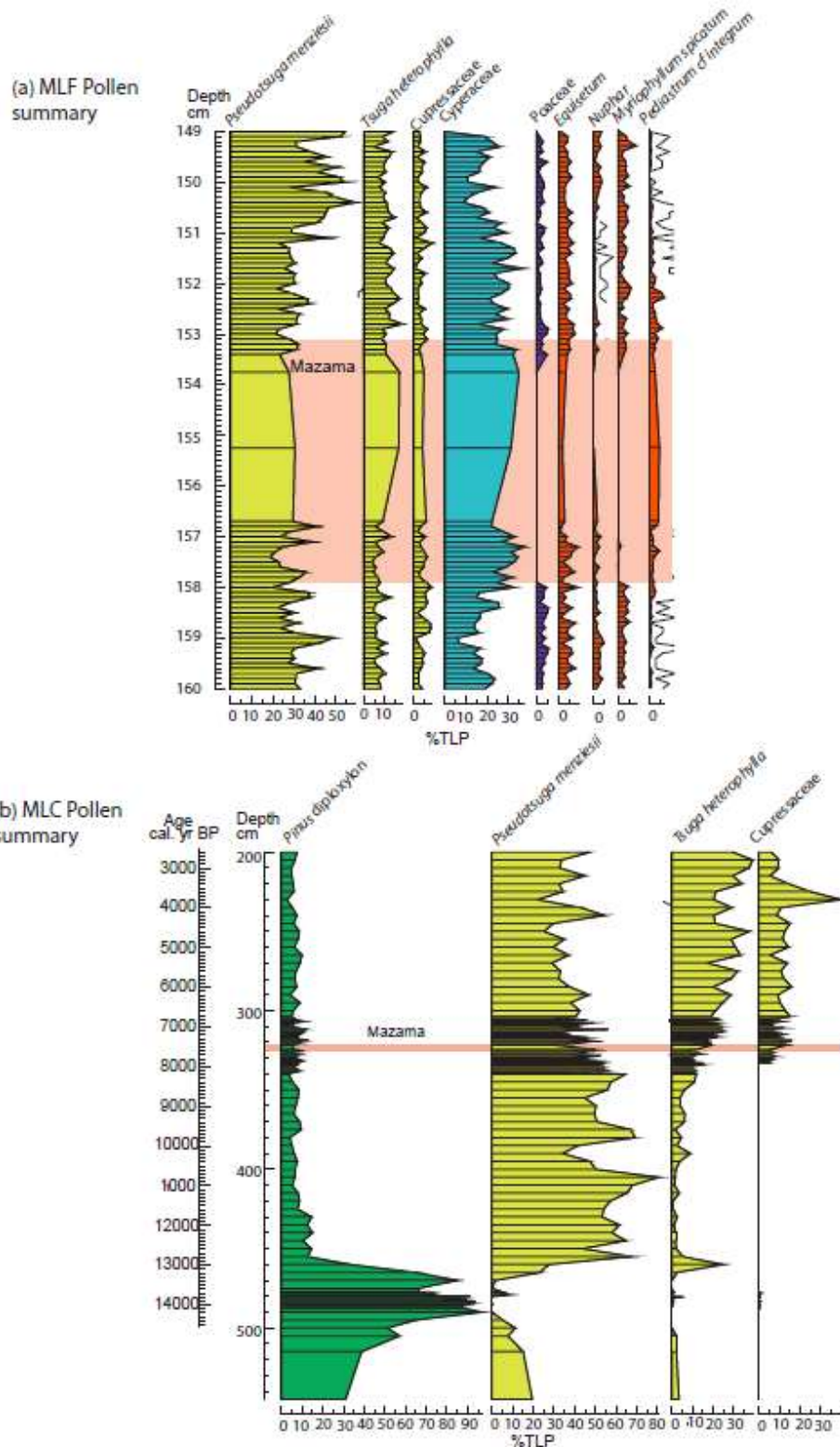


791 Figure 5: Diatom assemblage from Moss Lake central displaying the lithology, percentage of  
792 diatoms, summary diagram, diatom zonation, diatom concentration and PCA axis 1 and 2.  
793 The shaded bar represents the location of the Mazama tephra (MLC-T324), also labelled. The  
794 solid line on percentage diagram is 10x exaggeration.



796 Figure 6: Diatom assemblage from Moss Lake fringe displaying the lithology, percentage of  
797 diatoms, summary diagram, diatom zonation, diatom concentration and PCA axis 1 and 2.  
798 The shaded bar represents the location of the Mazama tephra (MLF-T158), also labelled. The  
799 solid line on percentage diagram is 10x exaggeration.





800

801 Figure 7: Summary pollen diagrams from (a) Moss Lake Fringe (MLF) and (b) Moss Lake  
 802 Central (MLC). Full pollen diagrams are presented in Egan *et al.*, (2016). Species coloured:  
 803 green= xerophytes, yellow= mesophyte, blue= hydrophyte, orange= spores and aquatic.

## Supplementary Material

Table 1: Geographical coordinates, topographical and limnological properties, water temperature, pH, conductivity and water chemistry for Swamp Lake and Moss Lake. Water chemistry includes the concentrations of: Total Organic Carbon (TOC), Total Carbon (TC), Inorganic Carbon (IC), Total Nitrates (TN), Chlorides, Nitrites, Nitrates, phosphates, Sulphates, Aluminium (Al), Calcium (Ca), Copper (Cu), Iron (Fe), Potassium (K), Lithium (Li), Magnesium (Mg), Manganese (Mn), Sodium (Na), Nickel (Ni), Lead (Pb) and Zinc (Zn).

Variable	Units	Moss Lake	
Latitude	(N)	47° 41' 35.7"	
Longitude	(w)	121° 50' 48.6"	
Distance from Mazama	(km)	530	
Altitude	(m asl)	158	
Max depth	(m)	4.5	
Area (approx.)	(m <sup>2</sup> )	13,275	
		July 2013	May 2014
pH		6.15	6.3
Conductivity	( $\mu\text{S cm}^{-1}$ )	14	22
Water temp	(°C)	-	18.3
TOC	(ppm)	15.07	-
TC	(ppm)	17.12	-
IC	(ppm)	2.049	-
TN	(ppm)	0.4697	-
Chloride	(ppm)	2.284	3.834
Nitrite	(ppm)	-	0.029
Nitrate	(ppm)	-	0.353
Phosphate	(ppm)	0.849	-
Sulphate	(ppm)	0.146	0.458
Al	(ppm)	0.28	0.163
Ca	(ppm)	4.035	2.741
Cu	(ppm)	0.011	0.012
Fe	(ppm)	0.281	0.061
K	(ppm)	1.692	0.046
Li	(ppm)	0.041	0.023
Mg	(ppm)	0.969	0.694
Mn	(ppm)	0.002	0.003
Na	(ppm)	2.254	1.412
Ni	(ppm)	0.002	0.005
Pb	(ppm)	0.011	0.01
Zn	(ppm)	0.253	0.02

Table 2. Locations and references of point provided in Figure 1 of the main document.

Point	Site name	Reference
1	Swamp Lake	(Street et al., 2012)
2	Osgood Swamp	(Adam, 1967)
3	Virgin Creek	(Davis, 1978)
4	Wildhorse Lake	(Blinman et al., 1979)
5	Wildcat Canyon	(Randle et al., 1971)
6	Upper Klamath Lake	(Bradbury et al., 2004)
7	Paisley Cave	(Preston et al., 1955)
8	Crater Lake Vicinity	(Bacon, 1983)
9	Sparks Lake	(Kittleman, 1973)
10	Diamond Lake	(Kittleman, 1973)
11	Toketee Falls	(Rubin & Alexander, 1960)
12	Fort Rock Cave	(Randle et al., 1971)
13	North Umpqua River Valley	(Bacon, 1983)
14	Paulina Lake	(Kittleman, 1973)
15	East Lake	(Kittleman, 1973)
16	Hobo Cave	(Randle et al., 1971)
17	Tumalo Lake	(Long et al., 2014)
18	Three Creek	(Long et al., 2014)
19	Round Lake	(Long et al., 2014)
20	Breitenbush Lake	(Long et al., 2014)
21	Lower Decker Lake	(Whitlock et al., 2011)
22	McCall Fen	(Doerner & Carrara , 2001)

23	Muir Creek	(Arnold and Libby, 1951; Crane, 1956; Kittleman, 1973; Valastro et al., 1968)
24	Lost Trail Pass Bog	(Blinman et al., 1979; Mehringer et al., 1977a)
25	Mount Rainer National Park	(Mullineaux, 1974)
26	Bear Swamp	(Blackford, Pers. Comm)
27	Davis Lake	(Barnosky, 1981)
28	Swamp Lake	(Blackford pers comm; Egan, Unpublished)
29	Covington	(Broecker et al., 1956)
30	Moss Lake	This paper
31	Bow Lake	(Rubin & Alexander, 1960)
32	Arrow Lake	(Rubin & Alexander, 1960)
33	Lake Washington	(Abella, 1988; Leopold et al., 1982)
34	Skykomish River	(Tabor et al., 1963)
35	Wildcat Lake	(Blinman et al., 1979)
36	Bogachiel River	(Heusser, 1983)
37	Rithets Bog	(Lowdon & Blake, 1970)
38	Pike Lake	(James et al., 2009)
39	Maltby Lake	(James et al., 2009)
40	Portage Inlet	(Buckley & Willis, 1970)
41	Bonaparte Meadows	(Mack et al., 1979)
42	Big Meadow Lake	(Powers & Wilcox, 1964)
43	Huff Lake	(Moseley et al., 1992)
44	Hager Lake	(Moseley et al., 1992)
45	Tepee Lake	(Mack et al., 1983)
46	Foy Lake	(Power et al., 2011)



47	Swiftcurrent Lake	(MacGregor et al., 2011)
48	Burnaby Lake	(Dyck et al., 1966)
49	Lake Mike	(Brown et al., 1989)
50	Marion Lake	(Mathewes, 1973)
51	Surprise Lake	(Mathewes, 1973)
52	Fraser Canyon	(Lowdon et al., 1969)
53	Squeah Lake	(Mathewes et al., 1972)
54	Lower Jaffre Lake	(Filippelli et al., 2006)
55	Drynoch Slide	(Sanger, 1967)
56	Drynoch Slide	(Lowdon et al., 1969)
57	Kilpoola Lake	(Heinrichs et al., 1999)
58	Green Lake	(Filippelli et al., 2006)
59	Dunn Peak	(Duford & Osborn, 1978)
60	Chase	(Lowdon & Blake, 1973)
61	Lavington	(Lowdon & Blake, 1970)
62	Deep Creek	(Dyck et al., 1965)
63	Lower Arrow Lake	(Dyck et al., 1965)
64	Mount Revelstoke	(Lowdon et al., 1971)
65	Cartwright Lake	(Beierle & Smith, 1998)
66	Copper Lake	(Beierle & Smith, 1998)
67	Johnson Lake	(Beierle & Smith, 1998)
68	Crowsnest Pass	(Driver, 1982)
69	Dog Lake	(Hallett et al., 1997)
70	Cobb Lake	(Hallett et al., 1997)
71	Upper Kananaskis Lake	(Beierle & Smith, 1998)

72	Frederick Lake	(Beierle & Smith, 1998)
73	Mary lake	(Hickman & Reasoner, 1994)
74	Opabin Lake	(Hickman & Reasoner, 1994)
75	Copper Lake	(White & Osborn, 1992)
76	Lake O'Hara	(Hickman & Reasoner, 1994)
77	Columbia River Valley	(Fulton, 1971)
78	Columbia River	(Buckley & Willis, 1969)
79	Tonquinn Pass	(Luckman et al., 1986)
80	Upper Pinto Fen	(Yu, 2007)
81	Goldeneye Lake Fen	(Yu, 2007)
82	Keephills Fen	(Chagué-Goff et al., 1996)
83	Quesnel Lake	(Gilbert & Desloges, 2012)
84	Nordans Pond Bog	(Pyne-O'Donnell et al., 2012)
85	Camp Century	(Hammer et al., 1980)
86	GISP 2	(Zdanowicz et al., 1999)

804

805

806

807 Full references:

808 Abella, S., (1988) The Effect of the Mt. Mazama Ashfall on the Planktonic Diatom Community of Lake  
809 Washington. *Limnology and oceanography*, 33(6, part 1), 1376–1385.

810 Adam, D.P., (1967) Late Pleistocene and recent palynology in the central Sierra Nevada, California. In  
811 J. Cushing & H. E. Wright, eds. *Quaternary Palaeoecology*. New Haven: Yale University Press.

812 Arnold, J.R. & Libby, W.F., (1951) Radiocarbon Dates. *Science*, 113(2927), 111–20.

813 Bacon, C.R., (1983) Eruptive history of Mount Mazama and Crater Lake Caldera, Cascade Range,  
814 U.S.A. *Journal of Volcanology and Geothermal Research*, 18(1-4), 57–115.

815 Barnosky, C.W., (1981) A record of late Quaternary vegetation from Davis Lake, southern Puget  
816 Lowland, Washington. *Quaternary Research*, 16(2), 221–239.

- 817 Beierle, B. & Smith, D.G., (1998) Severe drought in the early Holocene (10,000–6800 BP) interpreted  
818 from lake sediment cores, southwestern Alberta, Canada. *Palaeogeography,*  
819 *Palaeoclimatology, Palaeoecology*, 140(1-4), 75–83.
- 820 Blinman, E., Mehringer, P.J. & Sheppard, J.C., (1979) Pollen influx and the deposition of Mazama and  
821 Glacier Peak tephra. In P. . . Sheets & D. . Grayson, eds. *Volcanic Activity and Human Ecology*.  
822 London: Academic Press Inc, pp. 393–425.
- 823 Broecker, W.S., Kulp, J.L. & Tucek, C.S., (1956) Lamont Natural Radiocarbon Measurements III.  
824 *Science*, 124(3223), 630.
- 825 Brown, T.A., Nelson, D.E., Mathewes, R.W., Vogel, J.S. & Southon, J.R., (1989) Radiocarbon dating of  
826 pollen by accelerator mass spectrometry. *Quaternary Research*, 32(2), 205–212.
- 827 Buckley, J.D. & Willis, E.H., (1970) Isotopes radiocarbon measurements VIII. *Radiocarbon*, 11, 87–  
828 129.
- 829 Buckley, J.D. & Willis, E.H., (1969) ISOTOPES' radiocarbon measurements VII. *Radiocarbon*, 11(1), 53–  
830 105.
- 831 Chagué-Goff, C., Goodarzi, F. & Fyfe, W.S., (1996) Elemental Distribution and Pyrite Occurrence in a  
832 Freshwater Peatland, Alberta. *The Journal of Geology*, 104(6), 649–663.
- 833 Crane, H.R., (1956) University of Michigan Radiocarbon Dates I. *Science*, 124(3224), 664–72.
- 834 Davis, O., (1978) Quaternary tephrochronology of the Lake Lahonta area, Nevada and California. In  
835 *Nevada Archaeological Survey Research Paper 7*.
- 836 Doerner, J.P. & Carrara, P.E., (2001) Late Quaternary Vegetation and Climatic History of the Long  
837 Valley Area, West-Central Idaho, U.S.A. *Quaternary Research*, 56(1), 103–111.
- 838 Driver, J.C., (1982) Early Prehistoric Killing Of Bighorn Sheep In The Southeastern Canadian Rockies.  
839 *Plains Anthropologist*, 27(98, Part 1), 265–271.
- 840 Duford, J.M. & Osborn, G.D., (1978) Holocene and latest Pleistocene cirque glaciations in the  
841 Schuswap Highland, British Columbia. *Canadian Journal of Earth Sciences*, 15, 865–873.
- 842 Dyck, W., Fyles, J.G. & Blake, W., (1965) Geological Survey of Canada radiocarbon dates IV.  
843 *Radiocarbon*, 7(1), 24–46.
- 844 Dyck, W., Lowdon, J.A., Fyles, J.G. & Blake, W., (1966) Geological Survey of Canada radiocarbon dates  
845 V. *Radiocarbon*, 8(1), 96–127.
- 846 Filippelli, G.M., Souch, C., Menounos, B., Slater-Atwater, S., Timothy Jull, A.J. & Slaymaker, O., (2006)  
847 Alpine lake sediment records of the impact of glaciation and climate change on the  
848 biogeochemical cycling of soil nutrients. *Quaternary Research*, 66(1), 158–166.
- 849 Fulton, R.J., (1971) Radiocarbon geochronology of Southern British Columbia. In *Paper presented at*  
850 *Geological Survey Of Canada*. pp. 71–73.

- 851 Gilbert, R. & Desloges, J.R., (2012) Late glacial and Holocene sedimentary environments of Quesnel  
852 Lake, British Columbia. *Geomorphology*, 179, 186–196.
- 853 Hallett, D.J., Hills, L. V. & Clague, J.J., (1997) New accelerator mass spectrometry radiocarbon ages  
854 for the Mazama tephra layer from Kootenay National Park, British Columbia, Canada. *Canadian*  
855 *Journal of Earth Sciences*, 34(9), 1202–1209.
- 856 Hammer, C.U., Clausen, H.B. & Dansgaard, W., (1980) Greenland ice sheet evidence of post-glacial  
857 volcanism and its climatic impact. *Nature*, 288(5788), 230–235.
- 858 Heinrichs, M.L., Walker, I.R., Mathewes, R.W. & Hebda, R.J., (1999) Holocene chironomid-inferred  
859 salinity and paleovegetation reconstruction from Kilpoola Lake, British Columbia. *Géographie*  
860 *physique et Quaternaire*, 53(2), 211–221.
- 861 Heusser, L.E., (1983) Vegetational history of the northwestern United States including Alaska. In H. E.  
862 Wright Jr & S. E. Porter, eds. *Late-Quaternary environments of the United States: Volume 1 The*  
863 *Late Pleistocene*. London: Longman.
- 864 Hickman, M. & Reasoner, M.A., (1994) Diatom responses to late Quaternary vegetation and climate  
865 change, and to deposition of two tephtras in an alpine and a sub-alpine lake in Yoho National  
866 Park, British Columbia. *Journal of Paleolimnology*, 11(2), 173–188.
- 867 James, T., Gowan, E.J., Hutchinson, I., Clague, J.J., Barrie, J.V. & Conway, K.W., (2009) Sea-level  
868 change and paleogeographic reconstructions, southern Vancouver Island, British Columbia,  
869 Canada. *Quaternary Science Reviews*, 28(13-14), 1200–1216.
- 870 Kittleman, L.R., (1973) Mineralogy, Correlation, and Grain-Size Distributions of Mazama Tephra and  
871 Other Postglacial Pyroclastic Layers, Pacific Northwest. *Geological Society of America Bulletin*,  
872 84(9), 2957–2980.
- 873 Leopold, E.B., Nickmann, R., Hedges, J.I. & Ertel, J.R., (1982) Pollen and lignin records of late  
874 quaternary vegetation, lake washington. *Science*, 218(4579), 1305–7.
- 875 Long, C.J., Power, M.J., Minckley, T.A. & Hass, A.L., (2014) The impact of Mt Mazama tephra  
876 deposition on forest vegetation in the Central Cascades, Oregon, USA. *The Holocene*, 24(4),  
877 503–511.
- 878 Lowdon, J.A. & Blake, W., (1970) Geological Survey of Canada radiocarbon dates IX. *Radiocarbon*,  
879 12(1), 46–86.
- 880 Lowdon, J.A. & Blake, W., (1973) Geological survey of Canada Radiocarbon dates XIII. *Geological*  
881 *Survey of Canada*, Paper, 73–77.
- 882 Lowdon, J.A., Robertson, I.M. & Blake, W., (1971) Geological Survey of Canada Radiocarbon Dates XI.  
883 *Radiocarbon*, 13(2), 255–324.
- 884 Lowdon, J.A., Wilmeth, R. & Blake, W., (1969) Geological Survey of Canada radiocarbon dates VIII.  
885 *Radiocarbon*, 11(1), 22–42.
- 886 Luckman, B., Kearney, M., King, R. & Beaudoin, A., (1986) Revised <sup>14</sup>C age for St. Helens Y tephra at  
887 Tonquin Pass, British Columbia. *Canadian Journal of Earth Sciences*, 23, 734–736.

- 888 MacGregor, K.R., Riihimaki, C.A., Myrbo, A., Shapley, M.D. & Jankowski, K., (2011) Geomorphic and  
889 climatic change over the past 12,900yr at Swiftcurrent Lake, Glacier National Park, Montana,  
890 USA. *Quaternary Research*, 75(1), 80–90.
- 891 Mack, R.N., Rutter, N.W. & Valastro, S., (1979) Holocene vegetation history of the Okanogan Valley,  
892 Washington. *Quaternary Research*, 12(2), 212–225.
- 893 Mack, R.N., Rutter, N.W. & Valastro, S., (1983) Holocene vegetational history of the Kootenai River  
894 Valley, Montana. *Quaternary Research*, 20(2), 177–193.
- 895 Mathewes, R.W., (1973) A palynological study of postglacial vegetation changes in the University  
896 Research Forest, southwestern British Columbia. *Canadian Journal of Botany*, 51(11), 2085–  
897 2103.
- 898 Mathewes, R.W., Borden, C. & Rouse, G., (1972) New radiocarbon dates from the Yale area of the  
899 lower Fraser River canyon, British Columbia. *Canadian Journal of Earth Sciences*, 9(8), 1055–  
900 1057.
- 901 Mehringer, P.J., Arno, S.F. & Petersen, K.L., (1977) Postglacial History of Lost Trail Pass Bog,  
902 Bitterroot Mountains, Montana. *Arctic and Alpine Research*, 9(4), 345–368.
- 903 Moseley, R.K., Bursik, R.J. & Mehringer, P.J., (1992) Paleoecology of peatlands at Huff and Hager  
904 Lakes, Idaho Panhandle National Forest: FY92 year-end summary. *Conservation Data Center*,  
905 *Idaho Department of Fish and Game, Boise*.
- 906 Mullineaux, D.R., (1974) Pumice and other pyroclastic deposits in Mount Rainier National Park,  
907 Washington. *Geological Survey Bulletin*, 1326, 1–80.
- 908 Platt Bradbury, J., Colman, S.M. & Dean, W.E., (2004) Limnological and Climatic Environments at  
909 Upper Klamath Lake, Oregon during the past 45 000 years. *Journal of Paleolimnology*, 31(2),  
910 167–188.
- 911 Power, M.J., Whitlock, C. & Bartlein, P.J., (2011) Postglacial fire, vegetation, and climate history  
912 across an elevational gradient in the Northern Rocky Mountains, USA and Canada. *Quaternary*  
913 *Science Reviews*, 30(19-20), 2520–2533.
- 914 Powers, H.A. & Wilcox, R.E., (1964) Volcanic Ash from Mount Mazama (Crater Lake) and from Glacier  
915 Peak. *Science*, 144(3624), 1334–6.
- 916 Preston, R.S., Person, E. & Deevey, E.S., (1955) Yale Natural Radiocarbon Measurements II. *Science*,  
917 122(3177), 954–60.
- 918 Pyne-O'Donnell, S.D.F. et al., (2012) High-precision ultra-distal Holocene tephrochronology in North  
919 America. *Quaternary Science Reviews*, 52, 6–11.
- 920 Randle, K., Goles, G.G. & Kittleman, L.R., (1971) Geochemical and petrological characterization of ash  
921 samples from cascade range volcanoes. *Quaternary Research*, 1(2), 261–282.
- 922 Rubin, M. & Alexander, C., (1960) U.S. Geological Survey Radiocarbon Dates V. *American Journal of*  
923 *Science Radiocarbon Supplement*, 2, 129–185.

- 924 Sanger, D., (1967) Prehistory of the Pacific Northwest Plateau as Seen from the Interior of British  
925 Columbia. *American Antiquity*, 32(2), 186–197.
- 926 Street, J.H., Anderson, R.S. & Paytan, A., (2012) An organic geochemical record of Sierra Nevada  
927 climate since the LGM from Swamp Lake, Yosemite. *Quaternary Science Reviews*, 40, 89–106.
- 928 Tabor, R.W., Frizzell, J.V.A., Booth, D.B., Waitt, R.B., Whetten, J.T. & Zartman, R.E., (1963) Geologic  
929 Map Of The Skykomish River 30- By 60 Minute Quadrangle, Washington. *U.S. Department of*  
930 *the Interior, U.S. Geological Survey*, 1–67.
- 931 Valastro, S., Davis, E.M. & Rightmire, C.T., (1968) University of Texas at Austin radiocarbon dates VI.  
932 *Radiocarbon*, 10(2), 384–401.
- 933 White, J. & Osborn, G., (1992) Evidence for a Mazama-like tephra deposited ca. 10 000 BP at Copper  
934 Lake, Banff National Park, Alberta. *Canadian Journal of Earth Sciences*, 52–62.
- 935 Whitlock, C., Briles, C.E., Fernandez, M.C. & Gage, J., (2011) Holocene vegetation, fire and climate  
936 history of the Sawtooth Range, central Idaho, USA. *Quaternary Research*, 75(1), 114–124.
- 937 Yu, Z., (2007) Holocene Carbon Accumulation of Fen Peatlands in Boreal Western Canada: A Complex  
938 Ecosystem Response to Climate Variation and Disturbance. *Ecosystems*, 9(8), 1278–1288.
- 939 Zdanowicz, C.M., Zielinski, G.A. & Germani, M.S., (1999) Mount Mazama eruption: Calendrical age  
940 verified and atmospheric impact assessed. *Geology*, 27(7), 621–624.

941

942

943 Table 3: Conventional ( $^{14}\text{C}$  years BP) and calibrated (cal. years BP) radiocarbon ages for

944 MLF.

Lab no.	Depth (cm)	Material	Age ( $^{14}\text{C}$ years BP $\pm$ 1 SD)	Age range (cal. years BP 2 SD)
SUERC-52705	147	Organic sediment	5645 $\pm$ 36	6496-6319
SUERC- 55693	147	Organic sediment	5796 $\pm$ 38	6713-6491
	(re-submission)			
SUERC-52704	151	Organic sediment directly above MLF-T158	4948 $\pm$ 37	5745-5599
SUERC-55690	151	Organic sediment directly above MLF-T158	5705 $\pm$ 35	6626-6407
	(re-submission)			
SUERC-52703	161	Organic sediment below MLF-T158	7049 $\pm$ 41	7958-7795

945

946